

Shannon entropy in quasiparticle states of quantum chains

Wentao Ye¹ and Jiaju Zhang^{1,2*}

¹*Department of Physics, School of Science, Tianjin University,
135 Yaguan Road, Tianjin 300350, China*

²*Center for Joint Quantum Studies, School of Science, Tianjin University,
135 Yaguan Road, Tianjin 300350, China*

Abstract

We investigate the Shannon entropy of the total system and its subsystems, as well as the subsystem Shannon mutual information, in quasiparticle excited states of free bosonic and fermionic chains and the ferromagnetic phase of the spin-1/2 XXX chain. For single-particle and double-particle states, we derive various analytical formulas for free bosonic and fermionic chains in the scaling limit. These formulas are also applicable to certain magnon excited states in the XXX chain in the scaling limit. We also calculate numerically the Shannon entropy and mutual information for triple-particle and quadruple-particle states in bosonic, fermionic, and XXX chains. We discover that Shannon entropy, unlike entanglement entropy, typically does not separate for quasiparticles with large momentum differences. Moreover, in the limit of large momentum difference, we obtain universal quantum bosonic and fermionic results that are generally distinct and cannot be explained by a semiclassical picture.

arXiv:2303.14132v2 [quant-ph] 15 Sep 2024

*Corresponding author: jiajuzhang@tju.edu.cn

Contents

1	Introduction	3
2	Free bosonic chain	7
2.1	Single-particle state $ k\rangle$	7
2.2	Double-particle state $ k^2\rangle$	7
2.3	Double-particle state $ k_1k_2\rangle$	8
2.3.1	Total system Shannon entropy	8
2.3.2	Subsystem Shannon entropy	9
2.3.3	Subsystem Shannon mutual information	10
3	Free fermionic chain	11
3.1	Single-particle state $ k\rangle$	11
3.2	Double-particle state $ k_1k_2\rangle$	12
3.2.1	Total system Shannon entropy	12
3.2.2	Subsystem Shannon entropy	12
3.2.3	Subsystem Shannon mutual information	13
4	XXX chain	14
4.1	Single-magnon state	15
4.2	Double-magnon state	15
4.2.1	Case I solution	15
4.2.2	Case II solution	15
4.2.3	Case IIIa solution	16
4.2.4	Case IIIb solution	17
5	States with three and four quasiparticles	19
6	Conclusion and discussion	22
A	States and probabilities in free bosonic chain	24
A.1	Quasiparticle excited states	25
A.2	Single-particle state $ k\rangle$	25
A.3	Double-particle state $ k^2\rangle$	26
A.4	Double-particle state $ k_1k_2\rangle$	27
B	States and probabilities in free fermionic chain	27
B.1	Quasiparticle excited states	27
B.2	Single-particle state $ k\rangle$	28
B.3	Double-particle state $ k_1k_2\rangle$	28

C States and probabilities in XXX chain	29
C.1 Magnon excited states	29
C.2 Single-magnon state	30
C.3 Double-magnon state	30
C.3.1 Case I solution	30
C.3.2 Case II solution	31
C.3.3 Case IIIa solution	31
C.3.4 Case IIIb solution	32
D SSH model	33
E Classical particles	34
E.1 Soft-core classical particles	34
E.1.1 One particle	34
E.1.2 Two identical particles	35
E.1.3 Two distinguishable particles	36
E.2 Hard-core classical particles	36
E.2.1 One particle	36
E.2.2 Two identical particles	37
E.2.3 Two distinguishable particles	38
E.3 Summary and generalization	38
F Shannon entropy of particle number probability distribution	40
F.1 Classical particles	40
F.2 Free bosonic chain	40
F.3 Free fermionic chain	41
G Shannon entropy in σ_j^x basis of XXX chain	41
G.1 The σ_j^x basis	41
G.2 Ground state	42
G.3 Single-magnon state	42

1 Introduction

Quasiparticles are interesting collective excitations in integrable many-body systems that often provide simple intuitive explanations for complex phenomena [1]. One such example is the entanglement entropy in quasiparticle states of integrable quantum spin chains, which displays intriguing universal features in the scaling limit [2–17]. It was found that under certain limits, the entanglement entropy in quasiparticle states displays universal behaviors that can be explained by a semiclassical quasiparticle picture [5, 6]. The aim of the paper is to investigate whether there exists a similar semiclassical picture for other quantities, such as the total system Shannon entropy, subsystem Shannon entropy,

and subsystem Shannon mutual information, in excited states of quasiparticles, akin to those observed for entanglement entropy.

In a state that is pure, the quantum correlation between a subsystem and its complement could be described by various entanglement measures, including the entanglement entropy, which refers to the von Neumann entropy of the reduced density matrix. Depending on the particular quantum state of a given many-body system, the entanglement entropy exhibits various behaviors in the scaling limit [18–22]. In this paper, we restrict our analysis to the bipartite case, where the entire system is divided into a subsystem A and its complement \bar{A} . A quasiparticle state could be represented by the momenta K of the excited quasiparticles, denoted as $|K\rangle$. The reduced density matrix of subsystem A can be denoted as $\rho_A = \text{tr}_{\bar{A}}|K\rangle\langle K|$, and the entanglement entropy can be calculated as $S_{A,K} = -\text{tr}_A(\rho_A \log \rho_A)$. It has been discovered that under the large energy condition

$$\max_{k \in K} \frac{1}{\varepsilon_k} \ll \min(\ell, L - \ell), \quad (1.1)$$

where ε_k is energy of the elementary excitation of one quasiparticle with momentum k , and the large momentum difference condition

$$|k - k'| \gg 1, \quad \forall k \in K, \forall k' \in K', \quad (1.2)$$

the entanglement entropy difference is given by [13]

$$S_{A,K \cup K'} - S_{A,K'} = -\text{tr}_A(\tilde{\rho}_{A,K} \log \tilde{\rho}_{A,K}), \quad (1.3)$$

where $\tilde{\rho}_{A,K}$ is an effective low-rank reduced density matrix. In other words, under the conditions (1.1) and (1.2), the spin chain with modes K' acts like a background, and contributions from the modes K to the entanglement entropy decouple from the background. Analytical formulas of the entanglement entropy difference in free bosonic and fermionic chains were obtained in [10, 11, 13], and these formulas and their proper combinations also apply to models with interactions such as spin-1/2 XXX chain and XXZ chain under certain conditions [13]. Furthermore, under the extra large momentum difference condition [10, 11]

$$|k_1 - k_2| \gg 1, \quad \forall k_1, k_2 \in K, k_1 \neq k_2, \quad (1.4)$$

the effective reduced density matrix $\tilde{\rho}_{A,K}$ has a simple semiclassical quasiparticle picture and the entanglement entropy difference (1.3) becomes the Shannon entropy of the probability distribution of the semiclassical quasiparticles [5, 6]. It was found recently that similar universal properties and semiclassical quasiparticle picture also apply to the subsystem distance in quasiparticle excited states of various quantum spin chains [9, 12, 23].

In quantum mechanics, one can express the state of a quantum system in a pure state $|\psi\rangle$ in any orthonormal basis $\{|i\rangle\}$ with $\langle i|j\rangle = \delta_{ij}$ as

$$|\psi\rangle = \sum_i c_i |i\rangle, \quad (1.5)$$

where the normalization of the state $\langle \psi|\psi\rangle = 1$ implies that $\{p_i = |c_i|^2\}$ forms a well-defined probability distribution, i.e., $p_i \geq 0$ and $\sum_i p_i = 1$. A quantum system in a mixed state is characterized by a

density matrix ρ , which is positive semi-definite and satisfies $\text{tr}\rho = 1$. One can write the density matrix in the orthonormal basis $\{|i\rangle\}$ as

$$\rho = \sum_{i,j} \rho_{ij} |i\rangle\langle j|, \quad (1.6)$$

and there is a well-defined probability distribution $\{p_i = \rho_{ii}\}$. The Shannon entropy [24, 25]

$$H = - \sum_i p_i \log p_i, \quad (1.7)$$

can be calculated for any arbitrary probability distribution $\{p_i\}$, which measures the uncertainty or randomness of the probability distribution. In the case of a quantum system in a pure or mixed state, the Shannon entropy depends on the chosen basis. In quantum spin chains, the direct product of the local basis at each individual site forms a natural basis. In the local basis, the Shannon entropy characterizes a type of interesting correlation between different parts of the quantum system. The Shannon entropy in the local basis of various quantum spin chains has been intensively studied for both the total system [26–32] and a subsystem [33–42]. The probabilities of finding different states in this basis are called formation probabilities [40]. These probabilities, especially the emptiness formation probability, have been the subject of extensive research [28, 34, 40, 43–55]. The Shannon entropy, which is dependent on the choice of basis, is more experimentally accessible than the basis-independent entanglement entropy. Measuring entanglement entropy in a general quantum state often necessitates the complex process of quantum state tomography [56], which can be challenging. In contrast, determining the Shannon entropy involves performing measurements in a chosen basis on multiple copies of the quantum state to obtain the probability distribution of outcomes, which can then be used to calculate the Shannon entropy.

In this paper, we examine the Shannon entropy of both the entire system and a connected subsystem in states of quasiparticle excitations of free bosonic and fermionic chains and the spin-1/2 XXX chain. We focus on translation invariant states, ensuring that the subsystem Shannon entropy remains independent of its position within the entire system and solely dependent on the subsystem size. We not only consider the single-particle and double-particle states, which facilitate analytical calculations, but also the states with more particles, for which we calculate the Shannon entropy using numerical methods. The results are then compared across diverse quantum spin chains and also with classical results. As depicted in Figure 1, we consider a connected subsystem $A = [1, \ell]$ with ℓ neighboring sites on a circular chain consisting of L sites. Only translation-invariant states in quantum spin chains and translation-invariant configurations in classical chains are taken into account. We compute the Shannon entropy of the entire system $H(L)$ and the subsystem Shannon entropy $H(\ell)$. Additionally, we evaluate the subsystem Shannon mutual information,

$$M(\ell) = H(\ell) + H(L - \ell) - H(L), \quad (1.8)$$

which is a measure of the correlation between the subsystem A and its complement B . Our focus is on understanding the behaviours in the total system Shannon entropy $H(L)$, the subsystem Shannon entropy $H(\ell)$, and the subsystem mutual information $I(\ell)$ as we approach the scaling limit $L \rightarrow +\infty$,

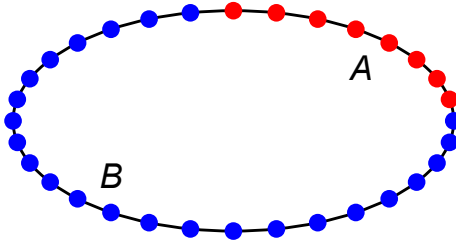


Figure 1: The spin chain consists of L sites arranged in a circle. We consider a connected subsystem A with ℓ adjacent sites, defined as $A = [1, \ell]$, and its complement $B = [\ell + 1, L]$.

$\ell \rightarrow +\infty$ while maintaining a constant ratio $x = \ell/L$. As there is the semiclassical picture for the entanglement entropy only in the large momentum difference limit [10, 11], we also take such a limit for the local basis Shannon entropy and see if there is a similar semiclassical picture.

In this paper, we present analytical formulas for the total and subsystem Shannon entropy and mutual information in single- and double-quasiparticle excited states of free bosonic and fermionic chains, as well as in single- and double-magnon excited states of the ferromagnetic phase of the spin-1/2 XXX chain. We also calculated numerically the Shannon entropy and mutual information in triple-particle and quadruple-particle states in the bosonic, fermionic and XXX chain. In the scaling limit where L and ℓ approach infinity with a fixed ratio between subsystem size and total system size $x = \ell/L$, both the total system Shannon entropy and subsystem Shannon entropy follow a universal logarithmic law, while the subsystem mutual information is a finite function of the ratio x . The results obtained for free bosonic and fermionic chains can also be applied to the XXX chain under certain circumstances. We compare our results with those of classical particles. In a single-particle state, the results are trivial and universal. In a general multi-particle state with large momentum differences, we find distinct universal bosonic and fermionic formulas that cannot be reproduced semiclassically. In the scaling limit, the contributions from different classical particles decouple, whereas this is not the case for quantum quasiparticles, even in the large momentum difference limit.

The rest of this paper is organized in the following way. In sections 2 and 3, we present calculations of the total system Shannon entropy and subsystem Shannon entropy and mutual information in quasiparticle excited states in free bosonic and fermionic chains, respectively. In section 4, we consider magnon excited states in the spin-1/2 XXX chain. In section 5, we evaluate numerically the Shannon entropy and mutual information in the triple-particle and quadruple-particle states in the bosonic, fermionic and XXX chains. The paper concludes with discussions in section 6. We collect the calculation details for free bosonic chain, free fermionic chain, and XXX chain in respectively appendices A, B and C. In appendix D, we discuss briefly the entanglement entropy and Shannon entropy in the Su-Schrieffer-Heeger (SSH) model. In appendix E, we consider the configurations of classical particles. In appendix F, we calculate the Shannon entropy for the probability distribution of subsystem particle numbers in free bosonic and fermionic chains. Finally, in appendix G, we study the Shannon entropy in the local basis of σ_j^x eigenstates of the XXX chain.

2 Free bosonic chain

In this section, we evaluate the total system and subsystem Shannon entropies and mutual information for the free bosonic chain in the single-particle state $|k\rangle$ and the double-particle states $|k^2\rangle$ and $|k_1 k_2\rangle$.

The quasiparticle states analyzed in this paper, within the context of free models, can be derived by considering the limit of infinite energy gap from the eigenstates of nearest-neighbor interacting models. In essence, free models can be regarded as particular instances of interacting models. The conclusions presented in this section, particularly the absence of semiclassical representations for the local basis Shannon entropy and mutual information, and the inability to isolate contributions from quasiparticles with large momentum difference, are valid for both the free bosonic chain discussed and the subsequent free fermionic chain. These findings also extend to their corresponding nearest-neighbor interacting models.

The construction of the quasiparticle states and the corresponding local configuration probabilities are shown in appendix A.

2.1 Single-particle state $|k\rangle$

In the state $|k\rangle$ with a single quasiparticle with momentum k , we get the Shannon entropy of the total system

$$H_k^{\text{bos}}(L) = \log L, \quad (2.1)$$

and the subsystem Shannon entropy

$$H_k^{\text{bos}}(\ell) = x \log L - (1-x) \log(1-x), \quad (2.2)$$

and the subsystem Shannon mutual information

$$M_k^{\text{bos}}(\ell) = -x \log x - (1-x) \log(1-x). \quad (2.3)$$

The results for the single-particle state $|k\rangle$ are the same with the results for the configuration of one classical particle (E.19), (E.20) and (E.21).

2.2 Double-particle state $|k^2\rangle$

We consider the state $|k^2\rangle$ with the mode of momentum k being excited twice. In the scaling limit, we get the Shannon entropy

$$H_{k^2}^{\text{bos}}(L) = 2 \log L - \log 2. \quad (2.4)$$

the subsystem Shannon entropy

$$H_{k^2}^{\text{bos}}(\ell) = 2x \log L - x(2-x) \log 2 - 2(1-x) \log(1-x), \quad (2.5)$$

and mutual information

$$M_{k^2}^{\text{bos}}(\ell) = -x^2 \log x^2 - 2x(1-x) \log[2x(1-x)] - (1-x)^2 \log(1-x)^2. \quad (2.6)$$

The results for the double-particle state $|k^2\rangle$ are the same as the results for the configuration of two identical classical particles (E.22), (E.23), and (E.24). It is easy to check that the results in the general r -particle state $|k^r\rangle = \frac{1}{\sqrt{r!}}(b_k^\dagger)^r|G\rangle$ are the same as the results for the configuration of r identical classical particles (E.28), (E.29), and (E.30). We skip the details of the calculation in this paper.

2.3 Double-particle state $|k_1 k_2\rangle$

In this subsection we calculate the Shannon entropy for the double-particle state $|k_1 k_2\rangle = b_{k_1}^\dagger b_{k_2}^\dagger|G\rangle$ in free bosonic chain.

2.3.1 Total system Shannon entropy

For general L and the momentum difference $k_{12} = k_1 - k_2$, we get the Shannon entropy of the total system

$$H_{k_1 k_2}^{\text{bos}}(L) = 2 \log L - 2 \log 2 + \frac{2 \log 2}{L} - \frac{4}{L} \sum_{j=1}^{L/2-1} \cos^2 \frac{\pi j k_{12}}{L} \log \cos^2 \frac{\pi j k_{12}}{L}. \quad (2.7)$$

For $|k_{12}| \ll L$ in the limit $L \rightarrow +\infty$, the Shannon entropy becomes

$$H_{k_1 k_2}^{\text{bos}}(L) = H_{k_1 k_2}^{\text{univ}}(L) = 2 \log L - 1, \quad (2.8)$$

which does not depend on the actual values of the momenta k_1, k_2 . As we will see in the subsequent section, the formula (2.8) also applies to the free fermionic chain under the condition $|k_{12}| \ll L$. So we also call it a universal result.

When $|k_{12}|$ is proportional to L in the scaling limit $L \rightarrow +\infty$, the Shannon entropy may take exceptional values for exceptional values of $|k_{12}|$. For $|k_{12}| = \frac{mL}{n} \leq \frac{L}{2}$ with the integer $n = 2, 3, 4, \dots$ being a divisor of L and the integer m being coprime with n , we get the total system Shannon entropy

$$\mathcal{H}_{k_1 k_2}^{\text{bos}}(L) = 2 \log L - 2 \log 2 - \frac{2}{n} \sum_{a=1}^{n-1} \cos^2 \frac{\pi a}{n} \log \cos^2 \frac{\pi a}{n}, \quad (2.9)$$

which is independent of m . Explicitly, for $n = \{2, 3, 4, 5, 6\}$, we get respectively

$$\begin{aligned} \mathcal{H}_{k_1 k_2}^{\text{bos}}(L) - 2 \log L = & \left\{ -2 \log 2, -\frac{4}{3} \log 2, -\frac{3}{2} \log 2, \right. \\ & -\frac{1}{5} \log 2 - \frac{1}{10} [(3 - \sqrt{5}) \log(3 - \sqrt{5}) + (3 + \sqrt{5}) \log(3 + \sqrt{5})], \\ & \left. -\frac{2}{3} \log 2 - \frac{1}{2} \log 3 \right\}. \end{aligned} \quad (2.10)$$

For a prime integer L , there is no $|k_{12}| = \frac{mL}{n} \leq \frac{L}{2}$ with coprime integers m, n , and so the formula (2.8) is valid for all k_{12} for a large prime integer L . Interestingly, in further $n \rightarrow +\infty$ limit, the exceptional formula (2.9) approaches the universal formula (2.8).

We have obtained three formulas for the total system Shannon entropy, i.e. the exact formula (2.7) written in terms of a summation which is valid for general L and k_{12} , the formula (2.8), i.e. the universal formula (2.8), which is valid for $|k_{12}| \ll L$ in the scaling limit, and the exceptional formula (2.9) which is valid for exceptional values of the momentum difference $|k_{12}| = \frac{mL}{n} \leq \frac{L}{2}$ with coprime integers m, n in the scaling limit. We show these results in Figure 2. In the left panel of Figure 2, we see that for

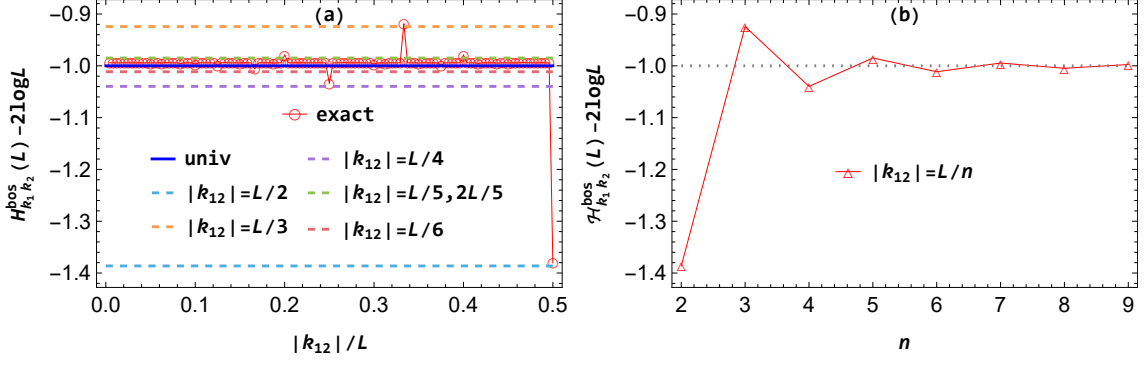


Figure 2: The Shannon entropy of the total system in the double-particle state $|k_1 k_2\rangle$ of the free bosonic chain. Left: The red empty circles connected with thin lines (exact) are the exact bosonic result (2.7) with $L = 240$. The dark blue solid line (univ) is the result (2.8), i.e. the universal formula (2.8), which is valid for $|k_{12}| \ll L$. The dashed lines are the exceptional result (2.9) which is valid for exceptional values of the momentum difference $|k_{12}| = \frac{mL}{n} \leq \frac{L}{2}$ with coprime integers m, n . Right: The large n limit of exceptional bosonic result (2.9) leads to the universal result (2.8).

most values of momentum difference $|k_{12}|$, not only for $|k_{12}| \ll L$, the Shannon entropy of the total system is (2.8), i.e. the universal formula (2.8). Only for a few exceptional values of $|k_{12}| = \frac{mL}{n} \leq \frac{L}{2}$ with coprime integers m, n , the Shannon entropy takes the exceptional form (2.9). In the right panel of Figure 2, it is shown that the $n \rightarrow +\infty$ limit of exceptional result (2.9) leads to the universal result (2.8).

2.3.2 Subsystem Shannon entropy

For general L , ℓ , and k_{12} , we get the exact subsystem Shannon entropy

$$\begin{aligned}
H_{k_1 k_2}^{\text{bos}}(\ell) = & - \left[(1-x)^2 + \frac{\sin^2(\pi k_{12} x)}{L^2 \sin^2 \frac{\pi k_{12}}{L}} \right] \log \left[(1-x)^2 + \frac{\sin^2(\pi k_{12} x)}{L^2 \sin^2 \frac{\pi k_{12}}{L}} \right] \\
& - \sum_{j=1}^{\ell} \left[\frac{2(1-x)}{L} - \frac{2 \sin(\pi k_{12} x) \cos \frac{2\pi k_{12}(j-\frac{\ell+1}{2})}{L}}{L^2 \sin \frac{\pi k_{12}}{L}} \right] \log \left[\frac{2(1-x)}{L} - \frac{2 \sin(\pi k_{12} x) \cos \frac{2\pi k_{12}(j-\frac{\ell+1}{2})}{L}}{L^2 \sin \frac{\pi k_{12}}{L}} \right] \\
& + \frac{2x}{L} (2 \log L - \log 2) - \sum_{j=1}^{\ell-1} (\ell-j) \frac{4}{L^2} \cos^2 \frac{\pi j k_{12}}{L} \log \left(\frac{4}{L^2} \cos^2 \frac{\pi j k_{12}}{L} \right). \tag{2.11}
\end{aligned}$$

For $|k_{12}| \ll L$ in the scaling limit $L \rightarrow +\infty$, $\ell \rightarrow +\infty$ with fixed $x = \ell/L$, we get the Shannon entropy

$$\begin{aligned}
H_{k_1 k_2}^{\text{bos}}(\ell) = & 2x \log L - 2x \log 2 - \left[(1-x)^2 + \frac{\sin^2(\pi k_{12} x)}{\pi^2 k_{12}^2} \right] \log \left[(1-x)^2 + \frac{\sin^2(\pi k_{12} x)}{\pi^2 k_{12}^2} \right] \\
& - 4 \int_0^{x/2} dy \left[(1-x) - \frac{\sin(\pi k_{12} x) \cos(2\pi k_{12} y)}{\pi k_{12}} \right] \log \left[(1-x) - \frac{\sin(\pi k_{12} x) \cos(2\pi k_{12} y)}{\pi k_{12}} \right] \\
& - 4 \int_0^{k_{12} x} \frac{dz}{k_{12}} \left(x - \frac{z}{k_{12}} \right) \cos^2(\pi z) \log \cos^2(\pi z). \tag{2.12}
\end{aligned}$$

For $1 \ll |k_{12}| \ll L$ in the scaling limit, we get the universal result

$$H_{k_1 k_2}^{\text{univ}}(\ell) = 2x \log L - 2(1-x) \log(1-x) - x^2 - 2x(1-x) \log 2, \tag{2.13}$$

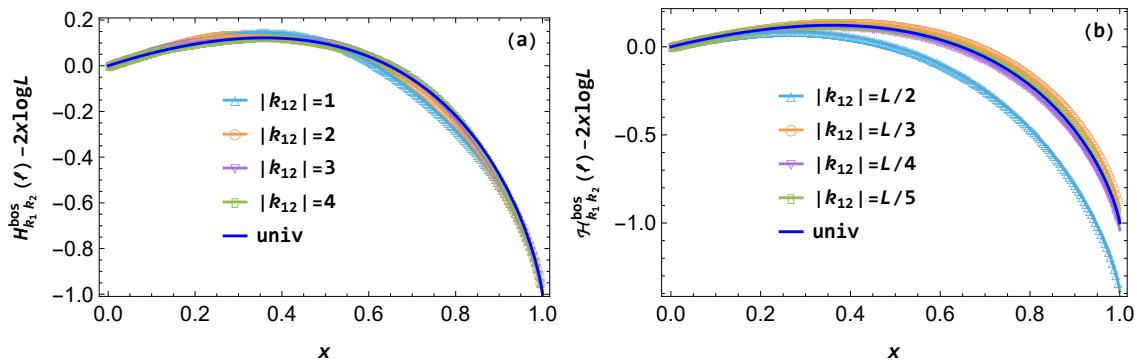


Figure 3: The subsystem Shannon entropy in the double-particle state $|k_1 k_2\rangle$ of the free bosonic chain. The empty symbols are the exact result (2.11) with $L = 240$. The dark blue solid lines are the universal result (2.13) which is valid for $1 \ll |k_{12}| \ll L$. In the left panel the other solid lines are the result (2.12) which is valid for $|k_{12}| \ll L$, and in the right panel the other solid lines are the exceptional result (2.14) which is valid for exceptional values $|k_{12}| = \frac{mL}{n} \leq \frac{L}{2}$ with coprime integers m, n .

which is not the same as either the result for two identical classical particles $H_{12}^c(\ell)$ (E.23) or the result for two distinguishable classical particles $H_{12}^d(\ell)$ (E.26). As we will see in the subsequent section, the universal result also applies to the double-particle state $|k_1 k_2\rangle$ in the free fermionic theory.

For exceptional values of the momentum difference $|k_{12}| = \frac{mL}{n} \leq \frac{L}{2}$ with coprime integers m, n in the scaling limit $L \rightarrow +\infty, \ell \rightarrow +\infty$ with fixed $x = \ell/L$, we get the exceptional value of the subsystem Shannon entropy

$$\mathcal{H}_{k_1 k_2}^{\text{bos}}(\ell) = 2x \log L - 2x \log 2 - 2(1-x) \log(1-x) - \frac{2x^2}{n} \sum_{a=1}^{n-1} \cos^2 \frac{\pi a}{n} \log \cos^2 \frac{\pi a}{n}. \quad (2.14)$$

Note that the $x \rightarrow 1$ limit of (2.14) is just (2.9) as it should be. Also, the $n \rightarrow +\infty$ limit of the exceptional result (2.14) leads to the universal result (2.13).

In summary, we have obtained four formulas for the subsystem Shannon entropy, i.e. the exact formula (2.11) which is valid for general L, ℓ , and k_{12} , the formula (2.12) which is valid for $|k_{12}| \ll L$ in the scaling limit $L \rightarrow +\infty, \ell \rightarrow +\infty$ with fixed $x = \ell/L$, the universal formula (2.13) which is valid for $1 \ll |k_{12}| \ll L$ in the scaling limit, the exceptional formula (2.14) which is valid for the exceptional values $|k_{12}| = \frac{mL}{n} \leq \frac{L}{2}$ with coprime integers m, n in the scaling limit. We show these results in Figure 3, where in the left panel we see the large $|k_{12}|$ limit of the bosonic result (2.12), which gives the universal result (2.13), and in the right panel we see the large n limit of the exceptional result (2.14), which also gives the universal result (2.13).

2.3.3 Subsystem Shannon mutual information

Using the results of the total system and subsystem Shannon entropies in different parameter regimes, we evaluate the subsystem Shannon mutual information. From (2.7) and (2.11), we obtain the exact mutual information $M_{k_1 k_2}^{\text{bos}}(\ell)$ that is valid for general L, ℓ, k_{12} . From (2.8) and (2.12), we obtain the mutual information

$$M_{k_1 k_2}^{\text{bos}}(\ell) = H_{k_1 k_2}^{\text{bos}}(\ell) + H_{k_1 k_2}^{\text{bos}}(L - \ell) - H_{k_1 k_2}^{\text{bos}}(L), \quad (2.15)$$

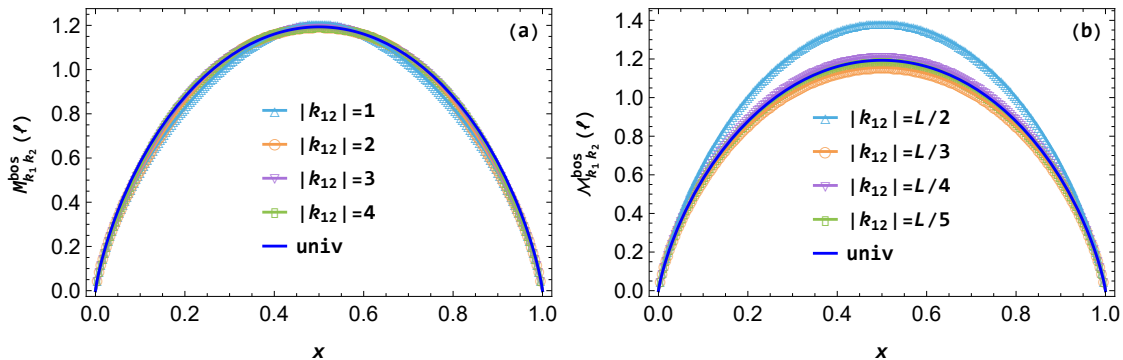


Figure 4: The subsystem Shannon mutual information in the double-particle state $|k_1 k_2\rangle$ of the free bosonic chain. The empty symbols are the exact result with $L = 240$. The dark blue solid lines are the universal result (2.16) which is valid for $1 \ll |k_{12}| \ll L$. In the left panel the other solid lines are the result which is valid for $|k_{12}| \ll L$, and in the right panel the other solid lines are the exceptional result (2.17) which is valid for the exceptional values $|k_{12}| = \frac{mL}{n} \leq \frac{L}{2}$ with coprime integers m, n .

which is valid for $|k_{12}| \ll L$ in the scaling limit. From (2.8) and (2.13), we further obtain the universal mutual information

$$M_{k_1 k_2}^{\text{univ}}(\ell) = -2x \log x - 2(1-x) \log(1-x) - 2x(1-x)(2 \log 2 - 1), \quad (2.16)$$

which is valid for $1 \ll |k_{12}| \ll L$ in the scaling limit. From (2.9) and (2.14), we obtain the exceptional mutual information

$$\mathcal{M}_{k_1 k_2}^{\text{bos}}(\ell) = -2x \log x - 2(1-x) \log(1-x) + \frac{4x(1-x)}{n} \sum_{a=1}^{n-1} \cos^2 \frac{\pi a}{n} \log \cos^2 \frac{\pi a}{n}, \quad (2.17)$$

which is valid for the exceptional values $|k_{12}| = \frac{mL}{n} \leq \frac{L}{2}$ with coprime integers m, n . In the scaling limit, the Shannon mutual information is a finite function of the ratio $x = \ell/L$. Surprisingly, both the results (2.16) and (2.17) are generally different from the result for two distinguishable classical particles $M_{12}^{\text{cl}}(\ell)$ (E.27). Only for the special case with $|k_{12}| = \frac{L}{2}$, there is $\mathcal{M}_{k_1 k_2}^{\text{bos}}(\ell) = M_{12}^{\text{cl}}(\ell)$. The results (2.16) and (2.17) are also different from the result for two identical classical particles $M_{12}^{\text{cl}}(\ell)$ (E.24). We show the subsystem Shannon mutual information in Figure 4.

3 Free fermionic chain

This section deals with the single-particle state $|k\rangle$ and double-particle state $|k_1 k_2\rangle$ in the free fermionic chain. The calculation details are collected in appendix B. The case of the free fermionic chain resembles that of the free bosonic chain, so we will keep it brief in this section.

3.1 Single-particle state $|k\rangle$

We can use the same calculations and results as for the single particle state $|k\rangle$ in the free bosonic chain in subsection 2.1. We will skip them here.

3.2 Double-particle state $|k_1 k_2\rangle$

This subsection deals with the calculation of Shannon entropy in the double-particle state $|k_1 k_2\rangle = b_{k_1}^\dagger b_{k_2}^\dagger |G\rangle$ in free fermionic chain.

3.2.1 Total system Shannon entropy

For general L and k_{12} , we get the Shannon entropy of the total system

$$H_{k_1 k_2}^{\text{fer}}(L) = 2 \log L - 2 \log 2 - \frac{4}{L} \sum_{j=1}^{L/2-1} \sin^2 \frac{\pi j k_{12}}{L} \log \sin^2 \frac{\pi j k_{12}}{L}. \quad (3.1)$$

For $|k_{12}| \ll L$ in the limit $L \rightarrow +\infty$, the Shannon entropy becomes

$$H_{k_1 k_2}^{\text{fer}}(L) = 2 \log L - 1, \quad (3.2)$$

which is the same as the bosonic result $H_{k_1 k_2}^{\text{bos}}(L)$ and the universal result $H_{k_1 k_2}^{\text{univ}}(L)$ in (2.8). This is why we call the expression a universal result.

For the exceptional value $|k_{12}| = \frac{mL}{n} \leq \frac{L}{2}$ with coprime integers m, n , we get the exceptional Shannon entropy

$$\mathcal{H}_{k_1 k_2}^{\text{fer}}(L) = 2 \log L - 2 \log 2 - \frac{2}{n} \sum_{a=1}^{n-1} \sin^2 \frac{\pi a}{n} \log \sin^2 \frac{\pi a}{n}. \quad (3.3)$$

Explicitly, for $n = \{2, 3, 4, 5, 6\}$, we get respectively

$$\begin{aligned} \mathcal{H}_{k_1 k_2}^{\text{fer}}(L) - 2 \log L = & \left\{ -2 \log 2, -\log 3, -\frac{3}{2} \log 2, \right. \\ & \log 2 - \frac{1}{10} [(5 - \sqrt{5}) \log(5 - \sqrt{5}) + (5 + \sqrt{5}) \log(5 + \sqrt{5})], \\ & \left. -\frac{2}{3} \log 2 - \frac{1}{2} \log 3 \right\}, \end{aligned} \quad (3.4)$$

which are generally different from the exceptional bosonic results (2.10). Again, in further large n limit, the exceptional result approaches the universal result.

We show these various results in Figure 5.

3.2.2 Subsystem Shannon entropy

For general L , ℓ , and k_{12} , we get the exact subsystem Shannon entropy

$$\begin{aligned} H_{k_1 k_2}^{\text{fer}}(\ell) = & - \left[(1-x)^2 - \frac{\sin^2(\pi k_{12} x)}{L^2 \sin^2 \frac{\pi k_{12}}{L}} \right] \log \left[(1-x)^2 - \frac{\sin^2(\pi k_{12} x)}{L^2 \sin^2 \frac{\pi k_{12}}{L}} \right] \\ & - \sum_{j=1}^{\ell} \left[\frac{2(1-x)}{L} + \frac{2 \sin(\pi k_{12} x) \cos \frac{2\pi k_{12}(j-\frac{\ell+1}{2})}{L}}{L^2 \sin \frac{\pi k_{12}}{L}} \right] \log \left[\frac{2(1-x)}{L} + \frac{2 \sin(\pi k_{12} x) \cos \frac{2\pi k_{12}(j-\frac{\ell+1}{2})}{L}}{L^2 \sin \frac{\pi k_{12}}{L}} \right] \\ & - \sum_{j=1}^{\ell-1} (\ell-j) \frac{4}{L^2} \sin^2 \frac{\pi j k_{12}}{L} \log \left(\frac{4}{L^2} \sin^2 \frac{\pi j k_{12}}{L} \right). \end{aligned} \quad (3.5)$$

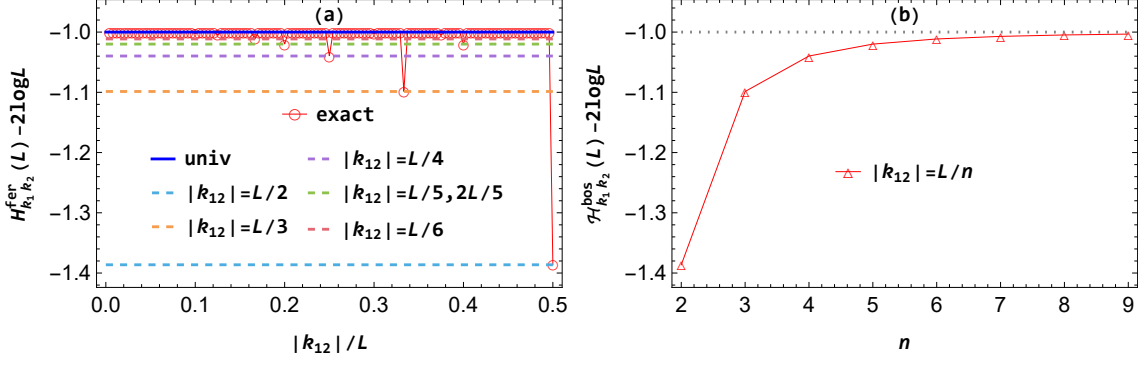


Figure 5: The Shannon entropy of the total system in the double-particle state $|k_1 k_2\rangle$ of the free fermionic chain. Left: The red empty circles connected with thin lines (exact) are the exact result (3.1) with $L = 240$. The dark blue solid line (univ) is the result (3.2), i.e. the universal formula (2.8), which is valid for $|k_{12}| \ll L$. The dashed lines are the exceptional result (3.3) which is valid for exceptional values of the momentum difference $|k_{12}| = \frac{mL}{n} \leq \frac{L}{2}$ with coprime integers m, n . Right: The large n limit of the exceptional result (3.3) leads to the universal result (2.8).

For $|k_{12}| \ll L$ in the scaling limit $L \rightarrow +\infty$, $\ell \rightarrow +\infty$ with fixed $x = \ell/L$, we get the Shannon entropy

$$\begin{aligned}
H_{k_1 k_2}^{\text{fer}}(\ell) &= 2x \log L - 2x \log 2 - \left[(1-x)^2 - \frac{\sin^2(\pi k_{12} x)}{\pi^2 k_{12}^2} \right] \log \left[(1-x)^2 - \frac{\sin^2(\pi k_{12} x)}{\pi^2 k_{12}^2} \right] \\
&\quad - 4 \int_0^{x/2} dy \left[(1-x) + \frac{\sin(\pi k_{12} x) \cos(2\pi k_{12} y)}{\pi k_{12}} \right] \log \left[(1-x) + \frac{\sin(\pi k_{12} x) \cos(2\pi k_{12} y)}{\pi k_{12}} \right] \\
&\quad - 4 \int_0^{k_{12} x} \frac{dz}{k_{12}} \left(x - \frac{z}{k_{12}} \right) \sin^2(\pi z) \log \sin^2(\pi z). \tag{3.6}
\end{aligned}$$

For $1 \ll k_{12} \ll L$ in the scaling limit, we get the universal result $H_{k_1 k_2}^{\text{univ}}(\ell)$ (2.13).

For exceptional values of the momentum difference $|k_{12}| = \frac{mL}{n} \leq \frac{L}{2}$ with coprime integers m, n in the scaling limit $L \rightarrow +\infty$, $\ell \rightarrow +\infty$ with fixed $x = \ell/L$, we get the subsystem Shannon entropy

$$\mathcal{H}_{k_1 k_2}^{\text{fer}}(\ell) = 2x \log L - 2x \log 2 - 2(1-x) \log(1-x) - \frac{2x^2}{n} \sum_{a=1}^{n-1} \sin^2 \frac{\pi a}{n} \log \sin^2 \frac{\pi a}{n}. \tag{3.7}$$

We show the various results in Figure 6.

3.2.3 Subsystem Shannon mutual information

With the results of the total system and subsystem Shannon entropies in different regimes of the parameters, we calculate the subsystem Shannon mutual information. From (3.1) and (3.5), we obtain the exact fermionic mutual information $M_{k_1 k_2}^{\text{fer}}(\ell)$ that is valid for general L, ℓ, k_{12} . From (3.2) and (3.6), we obtain

$$M_{k_1 k_2}^{\text{fer}}(\ell) = H_{k_1 k_2}^{\text{fer}}(\ell) + H_{k_1 k_2}^{\text{fer}}(L - \ell) - H_{k_1 k_2}^{\text{fer}}(L), \tag{3.8}$$

which is valid for $|k_{12}| \ll L$ in the scaling limit. From (3.2) and (2.13), we obtain the universal mutual information $M_{k_1 k_2}^{\text{univ}}(\ell)$ which is the same as (2.16) and is valid for $1 \ll |k_{12}| \ll L$ in the scaling limit. From (3.3) and (3.7), we obtain the exceptional mutual information

$$\mathcal{M}_{k_1 k_2}^{\text{fer}}(\ell) = -2x \log x - 2(1-x) \log(1-x) + \frac{4x(1-x)}{n} \sum_{a=1}^{n-1} \sin^2 \frac{\pi a}{n} \log \sin^2 \frac{\pi a}{n}, \tag{3.9}$$

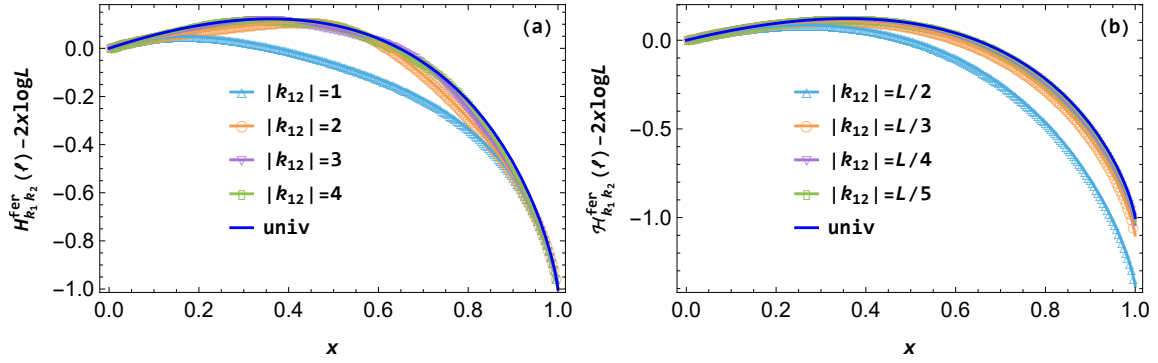


Figure 6: The subsystem Shannon entropy in the double-particle state $|k_1 k_2\rangle$ of the free fermionic chain. The empty symbols are the exact result (3.5) with $L = 240$. The dark blue solid lines are the universal result (2.13) which is valid for $1 \ll |k_{12}| \ll L$. In the left panel the other solid lines are the result (3.6) which is valid for $|k_{12}| \ll L$, and in the right panel the other solid lines are the exceptional result (3.7) which is valid for the exceptional values $|k_{12}| = \frac{mL}{n} \leq \frac{L}{2}$ with coprime integers m, n .

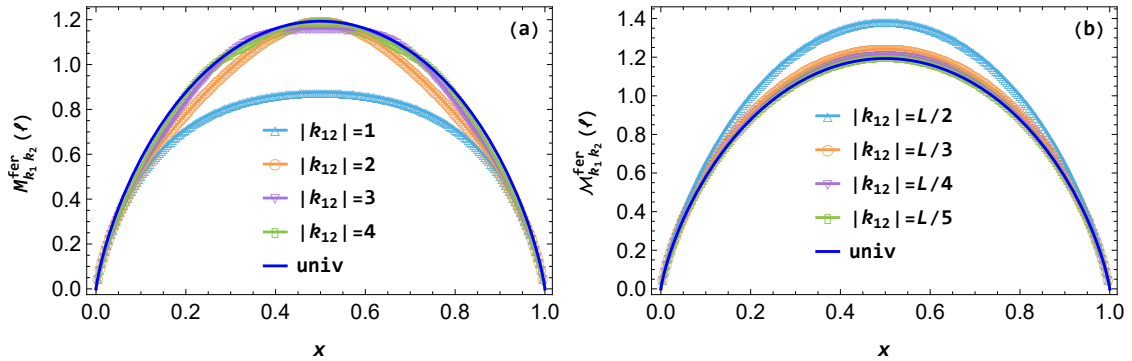


Figure 7: The subsystem Shannon mutual information in the double-particle state $|k_1 k_2\rangle$ of the free fermionic chain. The empty symbols are the exact result with $L = 240$. The dark blue solid lines are the universal result (2.16) which is valid for $1 \ll |k_{12}| \ll L$. In the left panel the other solid lines are the result (3.8) which is valid for $|k_{12}| \ll L$, and in the right panel the other solid lines are the exceptional result (3.9) which is valid for the exceptional values $|k_{12}| = \frac{mL}{n} \leq \frac{L}{2}$ with coprime integers m, n .

which is valid for the exceptional values of the momentum difference $|k_{12}| = \frac{mL}{n} \leq \frac{L}{2}$ with coprime integers m, n . We show the subsystem mutual information in Figure 7.

4 XXX chain

In this section, we compute the Shannon entropy of the total system and its subsystem and the subsystem mutual information in single- and double-magnon excited states of the spin-1/2 XXX chain. The single-magnon state results are identical to those for the single-particle states in free bosonic and fermionic chains. The double-magnon state is more complex, as it can be either a scattering state or a bound state. The total system Shannon entropy part in this section has overlaps with [32].

4.1 Single-magnon state

In the single-magnon state $|I\rangle$ total system Shannon entropy and the subsystem Shannon entropy and mutual information are the same as those of one-particle states in the free bosonic and fermionic chains in, respectively, subsections 2.1 and 3.1 and the configurations of one soft-core and hard-core classical particles in, respectively, subsections E.1.1 and E.2.1. We will not repeat the calculations here.

4.2 Double-magnon state

The double-magnon state $|I_1 I_2\rangle$ and corresponding configuration probabilities in XXX chain are shown in appendix C.

4.2.1 Case I solution

The total system Shannon entropy $H_{00}^I(L)$ and subsystem Shannon entropy $H_{00}^I(\ell)$ and mutual information $M_{00}^I(\ell)$ in state $|00\rangle$ are, respectively, the same as $H_{12}^{\text{hard}}(L)$ (E.12), $H_{12}^{\text{hard}}(\ell)$ (E.13), and $M_{12}^{\text{hard}}(\ell)$ (E.14). We will not repeat the calculations here.

4.2.2 Case II solution

From these probabilities, we obtain for general parameters L , ℓ , I_1 and I_2 the total system Shannon entropy and the subsystem Shannon entropy and mutual information

$$H_{I_1 I_2}^{\text{II}}(L) = - \sum_{1 \leq j_1 < j_2 \leq L} p_{j_1 j_2}^{\text{II}} \log p_{j_1 j_2}^{\text{II}}, \quad (4.1)$$

$$H_{I_1 I_2}^{\text{II}}(\ell) = -p_0^{A,\text{II}} \log p_0^{A,\text{II}} - \sum_{j=1}^{\ell} p_j^{A,\text{II}} \log p_j^{A,\text{II}} - \sum_{1 \leq j_1 < j_2 \leq \ell} p_{j_1 j_2}^{A,\text{II}} \log p_{j_1 j_2}^{A,\text{II}}, \quad (4.2)$$

$$M_{I_1 I_2}^{\text{II}}(\ell) = H_{I_1 I_2}^{\text{II}}(\ell) + H_{I_1 I_2}^{\text{II}}(L - \ell) - H_{I_1 I_2}^{\text{II}}(L), \quad (4.3)$$

where we have used the probabilities $p_{j_1 j_2}^{\text{II}}$ (C.17), $p_0^{A,\text{II}}$ (C.18), $p_j^{A,\text{II}}$ (C.19) and $p_{j_1 j_2}^{A,\text{II}}$ (C.20).

We are interested in how the above results (4.1), (4.2) and (4.3) behave in the scaling limit $L \rightarrow +\infty$, $\ell \rightarrow +\infty$ with fixed ratio $x = \ell/L$. We define the scaled Bethe numbers

$$\iota_1 = \lim_{L \rightarrow +\infty} \frac{I_1}{L}, \quad \iota_2 = \lim_{L \rightarrow +\infty} \frac{I_2}{L}. \quad (4.4)$$

When $\iota_1 = \iota_2 = 0$ or $\iota_1 = \iota_2 = 1$ or $\iota_1 = 0, \iota_2 = 1$, we have $\theta \rightarrow 0$ and obtain

$$\begin{aligned} \lim_{L \rightarrow +\infty} H_{I_1 I_2}^{\text{II}}(L) &= H_{k_1 k_2}^{\text{bos}}(L), & \lim_{L \rightarrow +\infty} H_{I_1 I_2}^{\text{II}}(\ell) &= H_{k_1 k_2}^{\text{bos}}(\ell), \\ \lim_{L \rightarrow +\infty} M_{I_1 I_2}^{\text{II}}(\ell) &= M_{k_1 k_2}^{\text{bos}}(\ell), & k_{12} &= I_{12}, \end{aligned} \quad (4.5)$$

with $H_{k_1 k_2}^{\text{bos}}(L)$ (2.8), $H_{k_1 k_2}^{\text{bos}}(\ell)$ (2.12) and $M_{k_1 k_2}^{\text{bos}}(\ell)$ (2.15) being the bosonic results in the scaling limit.

When $\iota_1 = \iota_2 \in (0, 1)$, we have $\theta \rightarrow \pi$ and the results approach to the fermionic results

$$\begin{aligned} \lim_{L \rightarrow +\infty} H_{I_1 I_2}^{\text{II}}(L) &= H_{k_1 k_2}^{\text{fer}}(L), & \lim_{L \rightarrow +\infty} H_{I_1 I_2}^{\text{II}}(\ell) &= H_{k_1 k_2}^{\text{fer}}(\ell), \\ \lim_{L \rightarrow +\infty} M_{I_1 I_2}^{\text{II}}(\ell) &= M_{k_1 k_2}^{\text{fer}}(\ell), & k_{12} &= I_{12} + 1, \end{aligned} \quad (4.6)$$

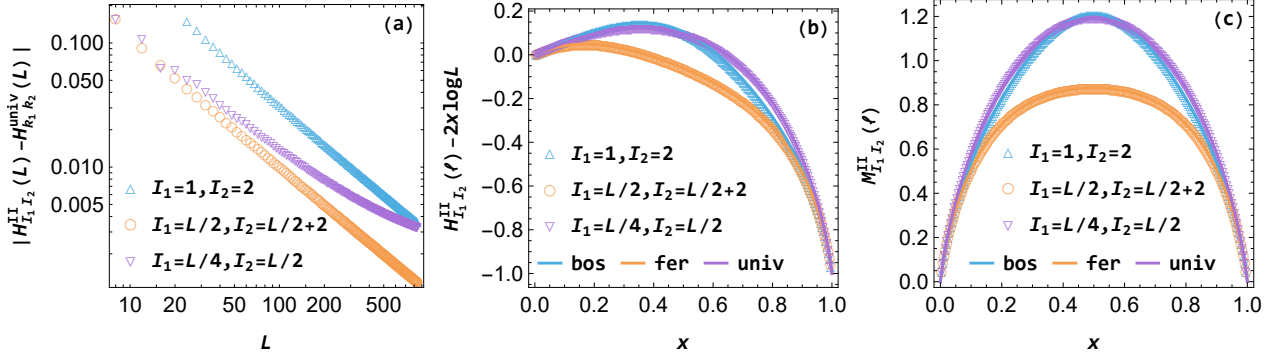


Figure 8: The total system Shannon entropy (left), subsystem Shannon entropy (middle) and mutual information (right) in the case II double-magnon state $|I_1 I_2\rangle$ of the XXX chain. The empty symbols are the exact numerical results. In the middle and right panels we have set $L = 240$ for the exact results, and the solid lines are the corresponding analytical results in the scaling limit, namely the bosonic (bos) results $H_{k_1 k_2}^{\text{bos}}(\ell)$ (2.12) and $M_{k_1 k_2}^{\text{bos}}(\ell)$ (2.15) with $|k_{12}| = 1$, fermionic (fer) results $H_{k_1 k_2}^{\text{fer}}(\ell)$ (3.6) and $M_{k_1 k_2}^{\text{fer}}(\ell)$ (3.8) with $|k_{12}| = 1$, and the universal results $H_{k_1 k_2}^{\text{univ}}(\ell)$ (2.13) and $M_{k_1 k_2}^{\text{univ}}(\ell)$ (2.16).

with $H_{k_1 k_2}^{\text{fer}}(L)$ (3.2), $H_{k_1 k_2}^{\text{fer}}(\ell)$ (3.6) and $M_{k_1 k_2}^{\text{fer}}(\ell)$ (3.8). When $0 \leq \iota_1 < \iota_2 \leq 1$, excluding the case $\iota_1 = 0, \iota_2 = 1$, we have $\theta \in [0, \pi)$ and the results approach to the universal results

$$\lim_{L \rightarrow +\infty} H_{I_1 I_2}^{\text{II}}(L) = H_{k_1 k_2}^{\text{univ}}(L), \quad \lim_{L \rightarrow +\infty} H_{I_1 I_2}^{\text{II}}(\ell) = H_{k_1 k_2}^{\text{univ}}(\ell), \quad \lim_{L \rightarrow +\infty} M_{I_1 I_2}^{\text{II}}(\ell) = M_{k_1 k_2}^{\text{univ}}(\ell), \quad (4.7)$$

with $H_{k_1 k_2}^{\text{univ}}(L)$ (2.8), $H_{k_1 k_2}^{\text{univ}}(\ell)$ (2.13) and $M_{k_1 k_2}^{\text{univ}}(\ell)$ (2.16). Note that the universal results do not depend on the actual values of the momenta k_1, k_2 . The exact numerical results of the total system Shannon entropy, subsystem Shannon entropy and mutual information, and the corresponding analytical results in the scaling limit are shown in Figure 8.

4.2.3 Case IIIa solution

From these probabilities, we obtain for general parameters L, ℓ , and I the total system Shannon entropy and the subsystem Shannon entropy and mutual information

$$H_{I_1 I_2}^{\text{IIIa}}(L) = - \sum_{1 \leq j_1 < j_2 \leq L} p_{j_1 j_2}^{\text{IIIa}} \log p_{j_1 j_2}^{\text{IIIa}}, \quad (4.8)$$

$$H_{I_1 I_2}^{\text{IIIa}}(\ell) = -p_0^{A, \text{IIIa}} \log p_0^{A, \text{IIIa}} - \sum_{j=1}^{\ell} p_j^{A, \text{IIIa}} \log p_j^{A, \text{IIIa}} - \sum_{1 \leq j_1 < j_2 \leq \ell} p_{j_1 j_2}^{A, \text{IIIa}} \log p_{j_1 j_2}^{A, \text{IIIa}}, \quad (4.9)$$

$$M_{I_1 I_2}^{\text{IIIa}}(\ell) = H_{I_1 I_2}^{\text{IIIa}}(\ell) + H_{I_1 I_2}^{\text{IIIa}}(L - \ell) - H_{I_1 I_2}^{\text{IIIa}}(L), \quad (4.10)$$

with the probabilities $p_{j_1 j_2}^{\text{IIIa}}$ (C.27), $p_0^{A, \text{IIIa}}$ (C.28), $p_j^{A, \text{IIIa}}$ (C.29) and $p_{j_1 j_2}^{A, \text{IIIa}}$ (C.30).

For finite v in the limit $L \rightarrow +\infty$, we have the tightly bound limit of the Shannon entropies and mutual information

$$H_{I_1 I_2}^{\text{IIIa}}(L) = \log L - \log(2 \sinh v) + v \coth v, \quad (4.11)$$

$$H_{I_1 I_2}^{\text{IIIa}}(\ell) = x[\log L - \log(2 \sinh v) + v \coth v] - (1 - x) \log(1 - x), \quad (4.12)$$

$$M_{I_1 I_2}^{\text{IIIa}}(\ell) = -x \log x - (1 - x) \log(1 - x). \quad (4.13)$$

Note that the total system Shannon entropy (4.11) has been obtained in [32].¹ Although the bound state has finite width $1/v$, the mutual information (4.13) does not depend on v . Further $v \rightarrow +\infty$ limit leads to the single-particle results

$$H_{I_1 I_2}^{\text{IIIa}}(L) = \log L, \quad (4.14)$$

$$H_{I_1 I_2}^{\text{IIIa}}(\ell) = x \log L - (1-x) \log(1-x), \quad (4.15)$$

$$M_{I_1 I_2}^{\text{IIIa}}(\ell) = -x \log x - (1-x) \log(1-x). \quad (4.16)$$

For $v = \frac{u}{L}$ with finite u , which leads to

$$u = - \lim_{L \rightarrow +\infty} L \log \left| \cos \frac{\pi I}{L} \right|, \quad (4.17)$$

we get the loosely bound limit of the results

$$H_{I_1 I_2}^{\text{IIIa}}(L) = 2 \log L + \log \left(\frac{\sinh u}{u} - 1 \right) - 2 \log 2 - \frac{4}{\frac{\sinh u}{u} - 1} \int_0^{\frac{u}{2}} \frac{dy}{u} \sinh^2 y \log \sinh^2 y, \quad (4.18)$$

$$\begin{aligned} H_{I_1 I_2}^{\text{IIIa}}(\ell) &= 2x \log L + \left(x + \frac{\frac{\sinh(ux) \sinh[u(1-x)]}{u^2} - x(1-x)}{\frac{\sinh u}{u} - 1} \right) \log \left(\frac{\sinh u}{u} - 1 \right) - 2x \log 2 \\ &\quad - \left(1-x - \frac{\frac{\sinh(ux) \sinh[u(1-x)]}{u^2} - x(1-x)}{\frac{\sinh u}{u} - 1} \right) \log \left(1-x - \frac{\frac{\sinh(ux) \sinh[u(1-x)]}{u^2} - x(1-x)}{\frac{\sinh u}{u} - 1} \right) \\ &\quad - \frac{4}{\frac{\sinh u}{u} - 1} \int_0^{\frac{x}{2}} dy \left[\frac{\sinh[u(1-x)] \cosh(2uy)}{u} - (1-x) \right] \log \left[\frac{\sinh[u(1-x)] \cosh(2uy)}{u} - (1-x) \right] \\ &\quad - \frac{4}{\frac{\sinh u}{u} - 1} \int_0^x dy (x-y) \sinh^2 \left[u \left(y - \frac{1}{2} \right) \right] \log \sinh^2 \left[u \left(y - \frac{1}{2} \right) \right], \end{aligned} \quad (4.19)$$

$$M_{I_1 I_2}^{\text{IIIa}}(\ell) = H_{I_1 I_2}^{\text{IIIa}}(\ell) + H_{I_1 I_2}^{\text{IIIa}}(L - \ell) - H_{I_1 I_2}^{\text{IIIa}}(L). \quad (4.20)$$

We show the total system Shannon entropy, subsystem Shannon entropy and mutual information in the case IIIa double-magnon state $|I_1 I_2\rangle$ of the XXX chain, as well as their tightly bound and loosely bound limits, in Figure 9. We see that in the range $I/L \in (0, 0.5)$ the results of the loosely bound limit apply for relatively small $I/L \gtrsim 0$ while the results of the tightly bound limit apply for relatively large $I/L \lesssim 0.5$. For the total system and subsystem Shannon entropies, there is the range $0.1 \lesssim I/L \lesssim 0.3$ in which both the results of the loosely bound limit and the results of the tightly bound limit apply.

4.2.4 Case IIIb solution

We obtain for general parameters L , ℓ , and I the total system Shannon entropy and the subsystem Shannon entropy and mutual information

$$H_{I_1 I_2}^{\text{IIIb}}(L) = - \sum_{1 \leq j_1 < j_2 \leq L} p_{j_1 j_2}^{\text{IIIb}} \log p_{j_1 j_2}^{\text{IIIb}}, \quad (4.21)$$

$$H_{I_1 I_2}^{\text{IIIb}}(\ell) = -p_0^{A, \text{IIIb}} \log p_0^{A, \text{IIIb}} - \sum_{j=1}^{\ell} p_j^{A, \text{IIIb}} \log p_j^{A, \text{IIIb}} - \sum_{1 \leq j_1 < j_2 \leq \ell} p_{j_1 j_2}^{A, \text{IIIb}} \log p_{j_1 j_2}^{A, \text{IIIb}}, \quad (4.22)$$

$$M_{I_1 I_2}^{\text{IIIb}}(\ell) = H_{I_1 I_2}^{\text{IIIb}}(\ell) + H_{I_1 I_2}^{\text{IIIb}}(L - \ell) - H_{I_1 I_2}^{\text{IIIb}}(L). \quad (4.23)$$

¹In [32] there is q which is related to v defined in this paper as $q = e^{-v}$.

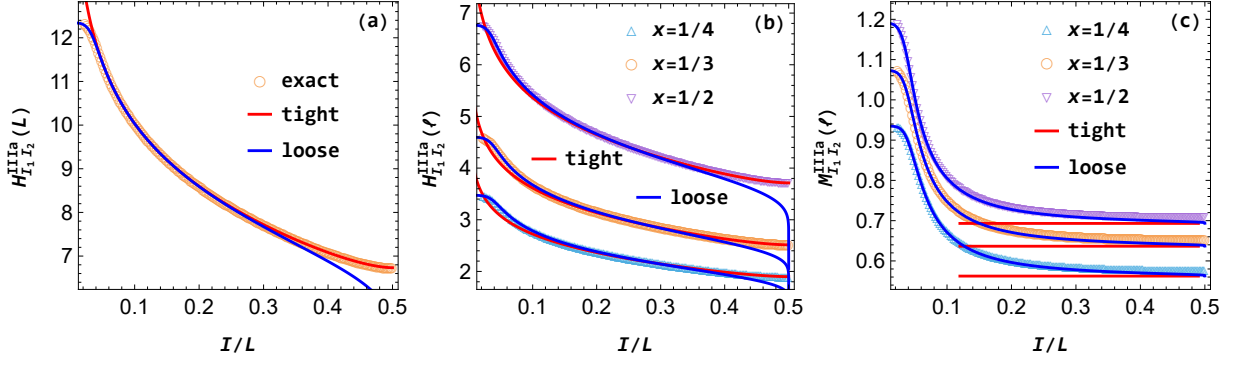


Figure 9: The total system Shannon entropy (left), subsystem Shannon entropy (middle) and mutual information (right) in the case IIIa double-magnon state $|I_1 I_2\rangle$ of the XXX chain. The empty symbols are the exact numerical results. The solid red and blue lines are, respectively, results of the tightly bound limit (4.11), (4.12) and (4.13), and results of the loosely bound limit (4.18), (4.19) and (4.20). We have set $L = 840$.

with the probabilities $p_{j_1 j_2}^{\text{IIIb}}$ (C.42), $p_0^{A, \text{IIIb}}$ (C.43), $p_j^{A, \text{IIIb}}$ (C.44) and $p_{j_1 j_2}^{A, \text{IIIb}}$ (C.45).

For finite v , we obtain the same tightly bound results as those in case IIIa states

$$H_{I_1 I_2}^{\text{IIIb}}(L) = \log L - \log(2 \sinh v) + v \coth v, \quad (4.24)$$

$$H_{I_1 I_2}^{\text{IIIb}}(\ell) = x[\log L - \log(2 \sinh v) + v \coth v] - (1-x) \log(1-x), \quad (4.25)$$

$$M_{I_1 I_2}^{\text{IIIb}}(\ell) = -x \log x - (1-x) \log(1-x). \quad (4.26)$$

Further $v \rightarrow +\infty$ limit leads to the single-particle results

$$H_{I_1 I_2}^{\text{IIIb}}(L) = \log L, \quad (4.27)$$

$$H_{I_1 I_2}^{\text{IIIb}}(\ell) = x \log L - (1-x) \log(1-x), \quad (4.28)$$

$$M_{I_1 I_2}^{\text{IIIb}}(\ell) = -x \log x - (1-x) \log(1-x). \quad (4.29)$$

For $v = \frac{u}{L}$ with fixed u in the scaling limit, we get the loosely bound limit of the results

$$H_{I_1 I_2}^{\text{IIIb}}(L) = 2 \log L + \log \left(\frac{\sinh u}{u} + 1 \right) - 2 \log 2 - \frac{4}{\frac{\sinh u}{u} + 1} \int_0^{\frac{u}{2}} \frac{dy}{u} \cosh^2 y \log \cosh^2 y, \quad (4.30)$$

$$\begin{aligned} H_{I_1 I_2}^{\text{IIIb}}(\ell) = & 2x \log L + \left(x + \frac{\frac{\sinh(ux) \sinh[u(1-x)]}{u^2} + x(1-x)}{\frac{\sinh u}{u} + 1} \right) \log \left(\frac{\sinh u}{u} + 1 \right) - 2x \log 2 \\ & - \left(1-x - \frac{\frac{\sinh(ux) \sinh[u(1-x)]}{u^2} + x(1-x)}{\frac{\sinh u}{u} + 1} \right) \log \left(1-x - \frac{\frac{\sinh(ux) \sinh[u(1-x)]}{u^2} + x(1-x)}{\frac{\sinh u}{u} + 1} \right) \\ & - \frac{4}{\frac{\sinh u}{u} + 1} \int_0^{\frac{x}{2}} dy \left[\frac{\sinh[u(1-x)] \cosh(2uy)}{u} + (1-x) \right] \log \left[\frac{\sinh[u(1-x)] \cosh(2uy)}{u} + (1-x) \right] \\ & - \frac{4}{\frac{\sinh u}{u} + 1} \int_0^x dy (x-y) \cosh^2 \left[u \left(y - \frac{1}{2} \right) \right] \log \cosh^2 \left[u \left(y - \frac{1}{2} \right) \right], \end{aligned} \quad (4.31)$$

$$M_{I_1 I_2}^{\text{IIIb}}(\ell) = H_{I_1 I_2}^{\text{IIIb}}(\ell) + H_{I_1 I_2}^{\text{IIIb}}(L - \ell) - H_{I_1 I_2}^{\text{IIIb}}(L). \quad (4.32)$$

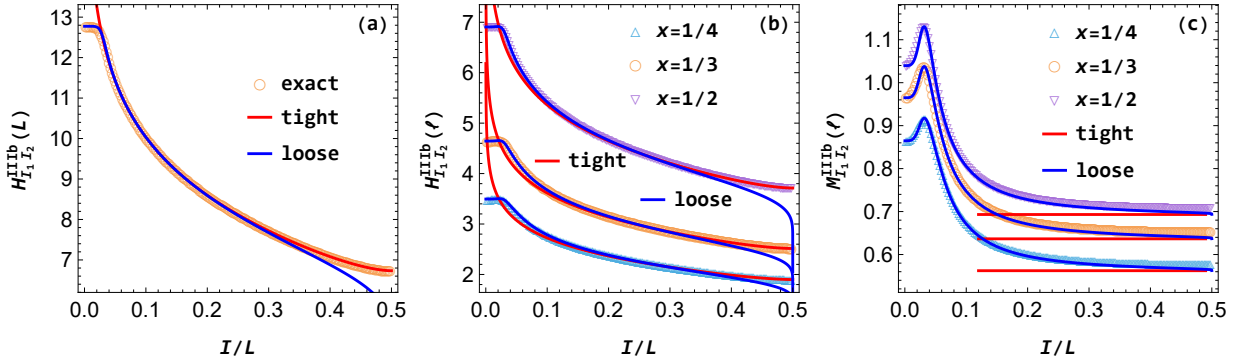


Figure 10: The total system Shannon entropy (left), subsystem Shannon entropy (middle) and mutual information (right) in the case IIIb double-magnon state $|I_1I_2\rangle$ of the XXX chain. The empty symbols are the exact numerical results. The solid red and blue lines are, respectively, the tightly bound results (4.24), (4.25) and (4.26), and the loosely bound results (4.30), (4.31) and (4.32). We have set $L = 840$.

A further $u \rightarrow 0$ limit of (4.30), (4.31), and (4.32) leads to

$$H_{I_1I_2}^{\text{IIIb}}(L) = 2 \log L - \log 2, \quad (4.33)$$

$$H_{I_1I_2}^{\text{IIIb}}(\ell) = 2x \log L - 2(1-x) \log(1-x) - x(2-x) \log 2, \quad (4.34)$$

$$M_{I_1I_2}^{\text{IIIb}}(\ell) = -x^2 \log x^2 - 2x(1-x) \log[2x(1-x)] - (1-x)^2 \log(1-x)^2, \quad (4.35)$$

which are the same as the results of two identical classical particles $H_{12}^{\text{cl}}(L)$ (E.22), $H_{12}^{\text{cl}}(\ell)$ (E.23), and $M_{12}^{\text{cl}}(\ell)$ (E.24). For $v = \frac{w}{L^2}$ with fixed w in the scaling limit, we get the same results (4.33), (4.34), and (4.35). In the limit where v approaches zero, known as the loosely bound limit, we can observe from equation (C.38) that p_1 becomes equal to p_2 and θ becomes zero. This implies that the two magnons exhibit behavior similar to two bosonic particles with identical momentum, which corresponds to the scenario analyzed in subsection 2.2. Consequently, this elucidates why the outcomes align with those obtained for two identical classical particles.

We show the total system Shannon entropy, subsystem Shannon entropy and mutual information in the case IIIb double-magnon state $|I_1I_2\rangle$ of the XXX chain, as well as their tightly and loosely bound limits, in Figure 10.

5 States with three and four quasiparticles

To verify the properties discovered for the double-particle states in the bosonic, fermionic, and XXX chains, in this section we calculate numerically the Shannon entropy and mutual information in states with three and four quasiparticles.

In the free bosonic chain we consider the triple-particle states $|k_1^2k_2\rangle$ and $|k_1k_2k_3\rangle$ and the quadruple-particle states $|k_1^3k_2\rangle$, $|k_1^2k_2^2\rangle$, $|k_1^2k_2k_3\rangle$ and $|k_1k_2k_3k_4\rangle$. In the free fermionic chain, we consider the triple-particle state $|k_1k_2k_3\rangle$ and the quadruple-particle state $|k_1k_2k_3k_4\rangle$. We set $k_i = 1 + (i-1)\delta k$ with $i = 1, 2, 3, 4$ and $\delta k = 1, 2, \dots$.

In the XXX chain, we consider the triple-magnon state $|\mathcal{I}_1\rangle$ with Bethe quantum numbers $\mathcal{I}_1 = (1, 1 + \delta I, 1 + 2\delta I)$ and $\delta I = 1, 3, 5$, which corresponds to the bosonic triple-particle state $|K_1\rangle$ with

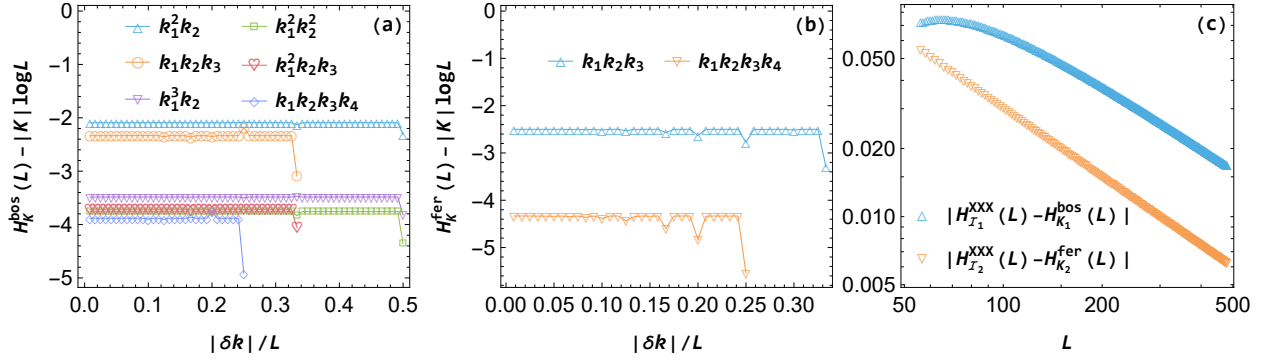


Figure 11: In the left and middle panels, we show the total system Shannon entropy in the triple-particle and quadruple-particle states of the free bosonic and fermionic chains, respectively. We have set $L = 120$ and $k_i = 1 + (i - 1)\delta k$ with $i = 1, 2, 3, 4$. In the right panel, we show the difference of total system Shannon entropy in the XXX chain and the corresponding result in the free bosonic/fermionic chain. For the state $\mathcal{I}_1 = (1, 2, 3)$, there is the corresponding bosonic state $K_1 = (1, 2, 3)$, and for the state $\mathcal{I}_2 = (\frac{L}{2}, \frac{L}{2} + 2, \frac{L}{2} + 4)$, there is the corresponding fermionic state $K_2 = (1, 2, 3)$.

$K_1 = (1, 1 + \delta k, 1 + 2\delta k)$ and $\delta k = \delta I$ in the scaling limit. We also consider the triple-magnon state $|\mathcal{I}_2\rangle$ with Bethe quantum numbers $\mathcal{I}_2 = (\frac{L}{2}, \frac{L}{2} + \delta I, \frac{L}{2} + 2\delta I)$ and $\delta I = 2, 4, 6$, which corresponds to the fermionic triple-particle state $|K_2\rangle$ with $K_2 = (1, 1 + \delta k, 1 + 2\delta k)$ and $\delta k = \delta I - 1$. Note the difference that in the bosonic chain $\delta k = \delta I$ and in the fermionic chain $\delta k = \delta I - 1$.

We present numerical results of the total system Shannon entropy in these triple- and quadruple-particle states in the left and middle panels of Figure 11. For each state, the total system Shannon entropy approaches a universal value for almost all values of δk , except for some exceptional cases when $\delta k/L$ has a finite numerator and denominator in the scaling limit. In both the bosonic and fermionic chains, the universal values for the states $|k_1 k_2 k_3\rangle$ and $|k_1 k_2 k_3 k_4\rangle$ are different, contrasting with the double-particle state $|k_1 k_2\rangle$ which has a universal quantum value. In the right panel of Figure 11, we compare the total system Shannon entropy in the XXX chain and the free bosonic/fermionic chain. We observe that in the scaling limit, the results for certain states in the XXX chain approach the corresponding values in the free bosonic/fermionic chain.

We show results of the subsystem Shannon entropy and mutual information in, respectively, figures 12 and 13. With the increase of the momentum difference δk , the subsystem Shannon entropy and mutual information approach some universal bosonic and fermionic values, as shown in panels (a), (b), (d) and (e) of figures 12 and panels (a), (b), (d) and (e) of figures 13, but the bosonic and fermionic values are generally distinct and also different from the results of classical particles, as shown in panels (c) and (f) of figures 12 and panels (c) and (f) of figures 13. In panels (a) and (b) of figures 12 and panels (a) and (b) of figures 13, we also show that results of certain states in the XXX chain approach the corresponding free bosonic/fermionic results.

The main conclusion of the paper is that there does not exist a classical description for the local basis Shannon entropy in quantum chains, as exemplified in the previous sections and this section. Additionally, it has been shown that contributions to the Shannon entropy from quasiparticles with large momentum differences do not separate.

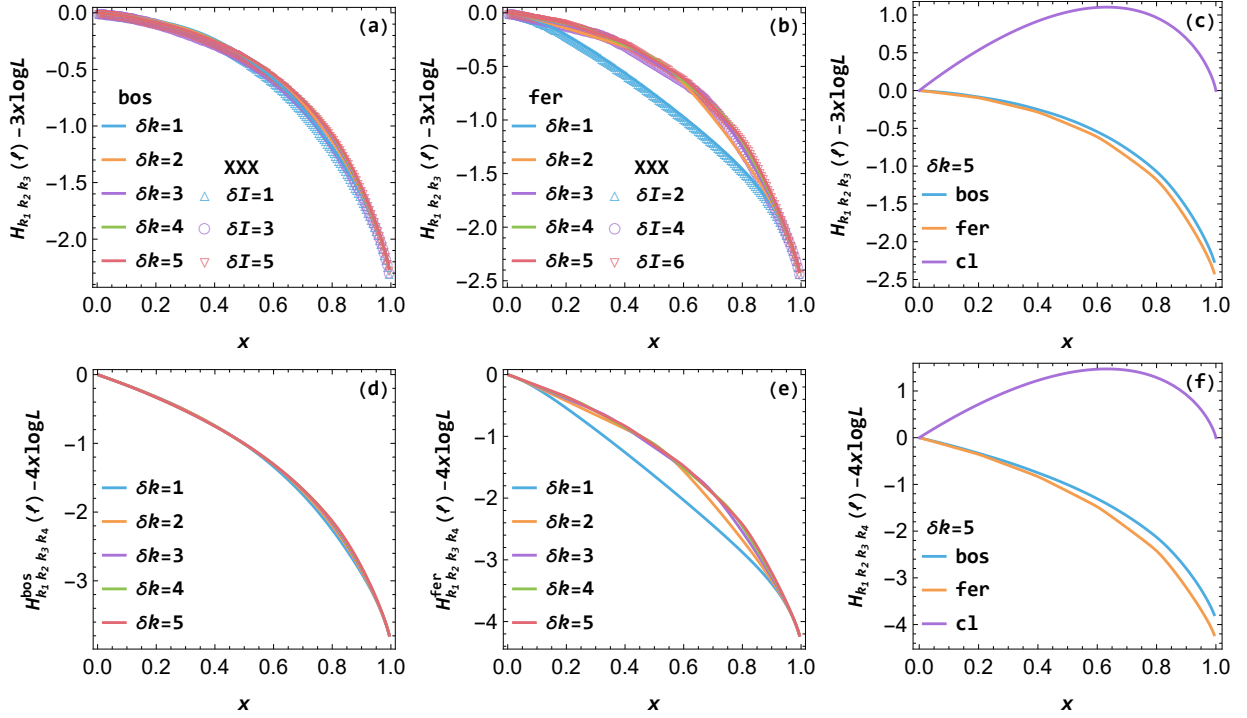


Figure 12: The subsystem Shannon entropy in triple-particle states (top panels) and quadruple-particle states (bottom panels) of the free bosonic and fermionic chains and the XXX chain. The length of the chain is $L = 180$.

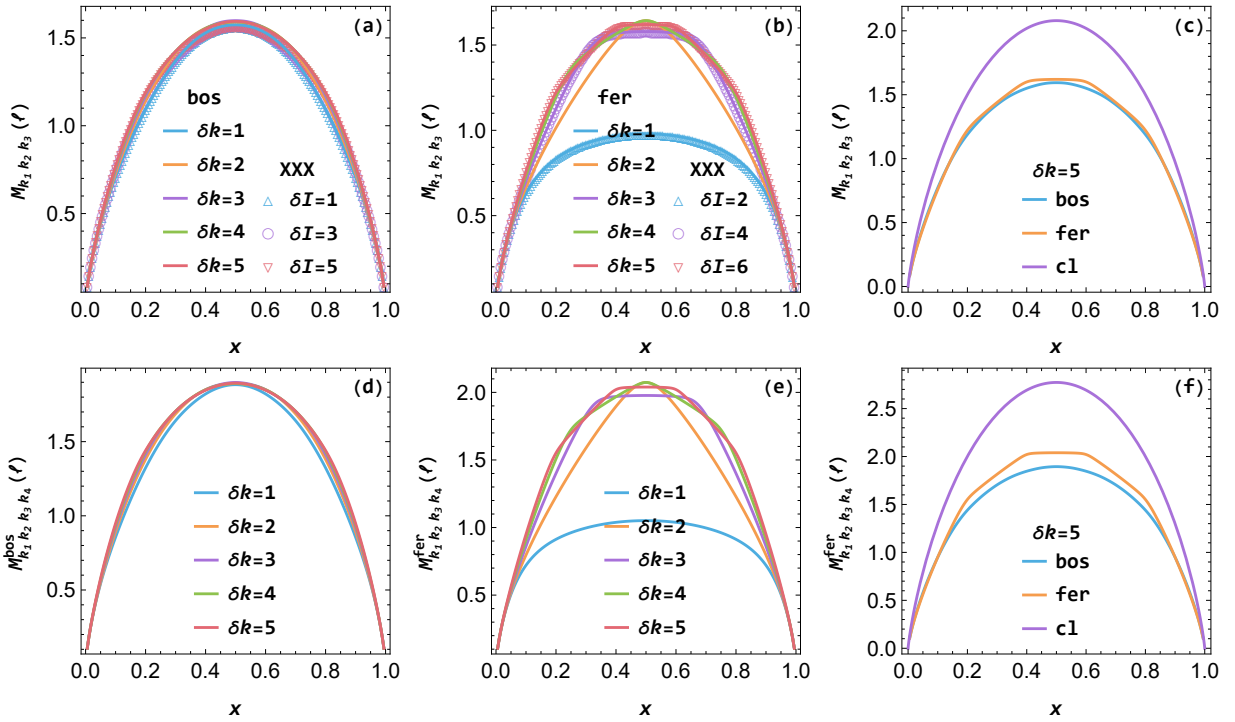


Figure 13: The subsystem Shannon mutual information in triple-particle states (top panels) and quadruple-particle states (bottom panels) of the free bosonic and fermionic chains and the XXX chain. We have used $L = 180$.

We denote a general quasiparticle excited state as $|K\rangle$ with K being the set of the momenta of the excited quasiparticles. The results for double-particle states in the previous sections and the results for triple- and quadruple-particle states in this section support the general form of the subsystem Shannon entropy in the scaling limit

$$H_K(\ell) = |K|x \log L + \delta H_K(x), \quad (5.1)$$

where $|K|$ is the total number of excited quasiparticles and $\delta H_K(x)$ is a function of the ratio $x = \ell/L$. On the right hand side of (5.1), the universal logarithmic divergent part is the same as that in the classical results (E.30) and (E.32), and this guarantees a finite subsystem Shannon mutual information in the scaling limit. For double-particle states, we have observed a universal quantum result in the limit $1 \ll |k_{12}| \ll L$

$$\delta H_{k_1 k_2}^{\text{bos}}(x) = \delta H_{k_1 k_2}^{\text{fer}}(x), \quad (5.2)$$

which is, however, generally *not* true for general triple- and quadruple-particle states. In the limit $1 \ll |k_{12}| \ll L$, there is the Shannon mutual information

$$M_{k_1 k_2}^{\text{bos}}(x) = M_{k_1 k_2}^{\text{fer}}(x), \quad (5.3)$$

which is also *not* true for general multi-particle states. Generally, in large momentum difference limit, there exist distinct universal bosonic and fermionic results, which are also different from the classical results.

6 Conclusion and discussion

In this paper we have presented an analysis of the total system Shannon entropy, subsystem Shannon entropy, and subsystem Shannon mutual information in quasiparticle excited states of free bosonic and fermionic chains, as well as the XXX chain. We compared the results across different spin chains and contrasted them with those of classical particles. Our findings indicate that, like the entanglement entropy, the formulas for the Shannon entropy in free bosonic and fermionic chains also apply to the Shannon entropy in the XXX chain, subject to certain limits. Additionally, we found that even when quasiparticles have large momentum differences, their contributions to the Shannon entropy do not decouple, unlike the entanglement entropy. In addition, we have discovered distinct universal bosonic and fermionic formulas for the total system Shannon entropy, subsystem Shannon entropy, and mutual information in the limit of large momentum differences, which are also distinct from any classical particle-based results. In other words, we did not observe any semiclassical quasiparticle picture that could reproduce the results of the Shannon entropy in quantum spin chains.

In Figure 14, we present the different results for the entanglement entropy, subsystem distance, and the local particle number basis Shannon entropy. For simplicity, we only calculated the Shannon entropy in free theories for fermionic and bosonic chains in this paper, which are a special case of the large energy condition. Unlike the entanglement entropy and subsystem distance, the Shannon entropy contributions from quasiparticles with large momentum differences do not decouple. As a result, the combined fermionic and bosonic results are generally not applicable to the XXX chain.

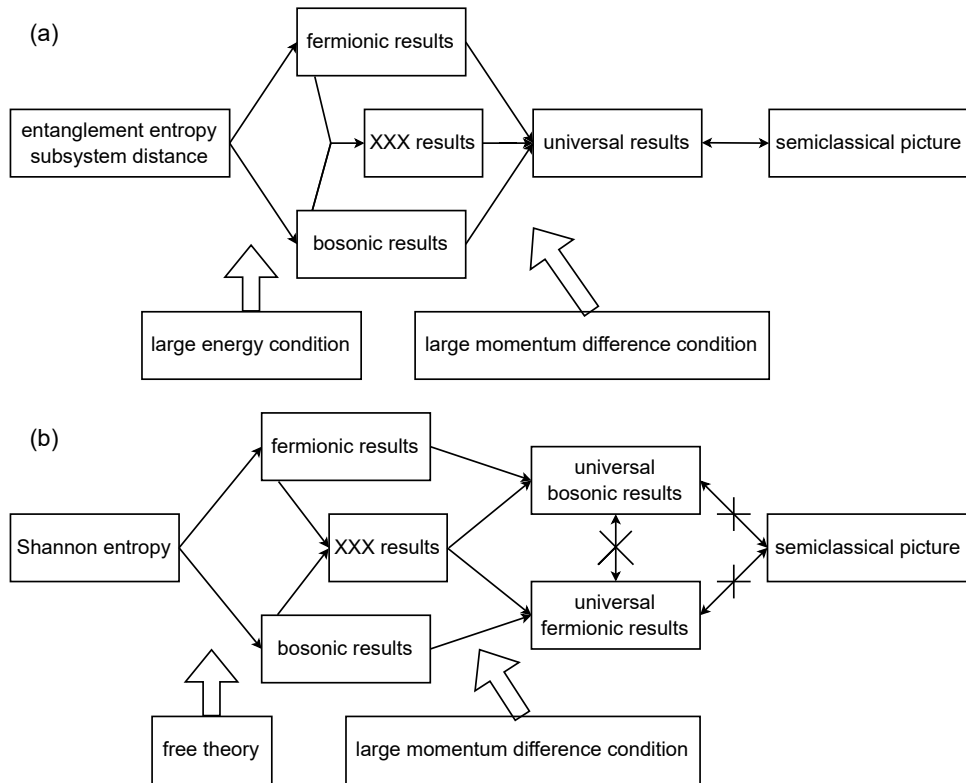


Figure 14: Summary of the different pictures for (a) the entanglement entropy and subsystem distance and (b) the Shannon entropy in the local particle number basis.

However, the fermionic and bosonic results can still be applied separately to the XXX chain within certain limits. Another notable distinction is that the semiclassical picture holds true for the universal entanglement entropy and subsystem distance, but it fails to explain the universal local particle number basis Shannon entropy.

In the main text of the paper, we have calculated the Shannon entropy using a particular basis of local states. It is essential to note that the definition of the Shannon entropy is dependent on the chosen basis. If one selects the eigenstates of the density matrix as the basis, the Shannon entropy will become equivalent to the von Neumann entropy for both pure and mixed quantum states of the total system or its subsystem. For quantum spin chains, the eigenstates of the subsystem particle number operator are also a natural basis. In Appendix F, we have studied the Shannon entropy of the subsystem particle number probability distribution in free bosonic and fermionic chains. We have found that the semiclassical quasiparticle picture applies in the large momentum difference limit. In Appendix G, we have calculated the Shannon entropy in the local basis of the σ_j^x eigenstates in the XXX chain. The results are significantly different from those obtained using the σ_j^z basis. Even in the single-magnon state, the σ_j^x basis Shannon entropy is already nontrivial. In certain limits, there exist forms of universal results for which no semiclassical quasiparticle picture applies.

We have found Shannon entropy in local bases for which no semiclassical quasiparticle picture applies. At the same time, there are the entanglement entropy, subsystem distance and Shannon entropy of the subsystem particle number probability distribution for which the semiclassical quasiparticle picture applies in the large momentum difference limit. We anticipate that the semiclassical picture applies

to coarse-grained properties but not to fine-grained properties. In other words, if one scrutinizes the microscopic details of a quasiparticle excited state, one can distinguish between quasiparticles and real particles. However, for a measure of certain macroscopic properties, quasiparticles behave similarly to real particles.

In our analysis, we have focused on models that encompass a single species of quasiparticles. In appendix D, we provide a concise discussion on the entanglement entropy and Shannon entropy within the context of the SSH model [57, 58], which incorporates two independent sets of fermionic modes. Our findings indicate that the individual contributions of these distinct fermionic species to both entanglement entropy and Shannon entropy are independent of each other. It would be of interest to investigate the behavior of Shannon entropy in alternative models that feature multiple species of quasiparticles. In this paper we have focused on translation invariant states in periodic chains. It would be interesting to consider states of inhomogeneous models such as open chains.

Experimental realization of excited states in spin chains was demonstrated in trapped atomic ion systems [59–61]. Recently, a proposal has been put forward to utilize neutral atom arrays to simulate fermionic many-body systems [62]. It would be fascinating to measure the Shannon entropy in quasiparticle excited states of spin chains and compare the experimental outcomes with the results presented in this paper. Within this context, measuring the Shannon entropy in quasiparticle excited states of spin chains offers a window into their quantum correlations. The Shannon entropy, as a quantitative measure of information content or uncertainty in a probability distribution, can provide insights into the distribution of quantum states in a system and how they evolve under various interactions and perturbations. Comparing the experimental outcomes with the theoretical predictions presented in this paper (or similar theoretical frameworks) would not only validate the accuracy of the experimental platform but also shed light on the microscopic mechanisms governing the quasiparticle dynamics. Furthermore, such experiments could potentially uncover novel quantum phenomena, such as unconventional quasiparticle statistics or emergent interactions.

Acknowledgements

We thank M. A. Rajabpour for reviewing an earlier version of the draft and providing valuable feedback and suggestions. JZ acknowledges the support from the National Natural Science Foundation of China (NSFC) through grant number 12205217.

A States and probabilities in free bosonic chain

In this appendix, we show calculation details for the free bosonic chain. We mainly show the constructions of the single-particle and double-particle excited states and the corresponding probabilities of subsystem configurations.

A.1 Quasiparticle excited states

The free bosonic chain has the Hamiltonian

$$H = \sum_{j=1}^L \left(a_j^\dagger a_j + \frac{1}{2} \right). \quad (\text{A.1})$$

We define the global modes

$$b_k^\dagger \equiv \frac{1}{\sqrt{L}} \sum_{j=1}^L e^{\frac{2\pi i j k}{L}} a_j^\dagger, \quad b_k \equiv \frac{1}{\sqrt{L}} \sum_{j=1}^L e^{-\frac{2\pi i j k}{L}} a_j, \quad k = 0, 1, \dots, L-1. \quad (\text{A.2})$$

The ground state is defined as

$$a_j |G\rangle = b_k |G\rangle = 0, \quad \forall j, \forall k. \quad (\text{A.3})$$

Using the global modes b_k^\dagger , one could construct the general translation-invariant global state

$$|k_1^{r_1} k_2^{r_2} \dots k_s^{r_s}\rangle = \frac{(b_{k_1}^\dagger)^{r_1} (b_{k_2}^\dagger)^{r_2} \dots (b_{k_s}^\dagger)^{r_s}}{\sqrt{r_1! r_2! \dots r_s!}} |G\rangle. \quad (\text{A.4})$$

In the free bosonic chain, the natural local basis at each site is the eigenstates of the operator of the excitation number. One could use the local modes a_j^\dagger to construct the general locally excited state

$$|j_1^{r_1} j_2^{r_2} \dots j_s^{r_s}\rangle = \frac{(a_{j_1}^\dagger)^{r_1} (a_{j_2}^\dagger)^{r_2} \dots (a_{j_s}^\dagger)^{r_s}}{\sqrt{r_1! r_2! \dots r_s!}} |G\rangle, \quad (\text{A.5})$$

which we will call local state for short. In the Hilbert space of the subsystem $A = [1, \ell]$, one has similarly the subsystem ground state $|G\rangle_A$ defined as

$$a_j |G\rangle_A = 0, \quad \forall j \in A, \quad (\text{A.6})$$

as well as the subsystem local excited states

$$|j_1^{r_1} j_2^{r_2} \dots j_s^{r_s}\rangle_A = \frac{(a_{j_1}^\dagger)^{r_1} (a_{j_2}^\dagger)^{r_2} \dots (a_{j_s}^\dagger)^{r_s}}{\sqrt{r_1! r_2! \dots r_s!}} |G\rangle_A, \quad j_1, j_2, \dots, j_s \in A. \quad (\text{A.7})$$

A.2 Single-particle state $|k\rangle$

We first consider the global single-particle state $|k\rangle = b_k^\dagger |G\rangle$, which could be written in terms of local states as

$$|k\rangle = \frac{1}{\sqrt{L}} \sum_{j=1}^L e^{\frac{2\pi i j k}{L}} |j\rangle. \quad (\text{A.8})$$

In state $|k\rangle$, there are L possible local states $|j\rangle$ with $j \in [1, L]$, and the corresponding probabilities are

$$p_j = \frac{1}{L}, \quad j \in [1, L]. \quad (\text{A.9})$$

For the subsystem A , there are $\ell + 1$ possible local states and the corresponding probabilities are listed in Table 1. The probabilities of the subsystem local states in Table 1 could be calculated either as the diagonal entries of the reduced density matrix in the local basis or as marginal probabilities of

the probability distribution (A.9) of the whole system. In this paper we will adopt the latter approach. Explicitly, we have used

$$\begin{aligned}
p_{A,0} &= \sum_{j=\ell+1}^L p_j, \\
p_{A,j} &= p_j, \quad j \in [1, \ell].
\end{aligned}
\tag{A.10}$$

local states	probabilities	ranges	numbers
$ G\rangle_A$	$p_{A,0} = 1 - x$	-	1
$ j\rangle_A$	$p_{A,j} = \frac{1}{L}$	$j \in [1, \ell]$	ℓ

Table 1: The local states and probabilities of the subsystem A in the single particle state $|k\rangle$ of the free bosonic chain. We have used $x = \frac{\ell}{L}$.

A.3 Double-particle state $|k^2\rangle$

In terms of the local states, the global double-particle state $|k^2\rangle = \frac{1}{\sqrt{2}}(b_k^\dagger)^2|G\rangle$ could be written as

$$|k^2\rangle = \frac{1}{L} \sum_{j=1}^L e^{\frac{4\pi i j k}{L}} |j^2\rangle + \frac{\sqrt{2}}{L} \sum_{1 \leq j_1 < j_2 \leq L} e^{\frac{2\pi i k(j_1+j_2)}{L}} |j_1 j_2\rangle.
\tag{A.11}$$

There are $\frac{L(L+1)}{2}$ possible local states, and the probabilities are shown in Table 2, which are the same as the probabilities of the configuration of two identical classical soft-core particles in Table 8.

local states	probabilities	ranges	numbers
$ j^2\rangle$	$p_{j^2} = \frac{1}{L^2}$	$j \in [1, L]$	L
$ j_1 j_2\rangle$	$p_{j_1 j_2} = \frac{2}{L^2}$	$1 \leq j_1 < j_2 \leq L$	$\frac{L(L-1)}{2}$

Table 2: The local states and probabilities of the total system in the double-particle state $|k^2\rangle$ of the free bosonic chain.

For the subsystem A , there are $\frac{(\ell+1)(\ell+2)}{2}$ possible local states and the corresponding probabilities are shown in Table 3. The probabilities in Table 3 are actually the marginal probabilities of the probability distribution in Table 2.

local states	probabilities	ranges	numbers
$ G\rangle_A$	$p_{A,0} = (1 - x)^2$	-	1
$ j\rangle_A$	$p_{A,j} = \frac{2(1-x)}{L}$	$j \in [1, \ell]$	ℓ
$ j^2\rangle_A$	$p_{A,j^2} = \frac{1}{L^2}$	$j \in [1, \ell]$	ℓ
$ j_1 j_2\rangle_A$	$p_{A,j_1 j_2} = \frac{2}{L^2}$	$1 \leq j_1 < j_2 \leq \ell$	$\frac{\ell(\ell-1)}{2}$

Table 3: The local states and probabilities of the subsystem A in the double-particle state $|k^2\rangle$ of the free bosonic chain.

A.4 Double-particle state $|k_1 k_2\rangle$

The double-particle state $|k_1 k_2\rangle$ could be written in terms of local states as

$$|k_1 k_2\rangle = \frac{\sqrt{2}}{L} \sum_{j=1}^L e^{\frac{2\pi i j(k_1+k_2)}{L}} |j^2\rangle + \frac{2}{L} \sum_{1 \leq j_1 < j_2 \leq L} e^{\frac{\pi i}{L}(j_1+j_2)(k_1+k_2)} \cos \frac{\pi j_{12} k_{12}}{L} |j_1 j_2\rangle, \quad (\text{A.12})$$

with the shorthand $j_{12} \equiv j_1 - j_2$ and $k_{12} \equiv k_1 - k_2$. As there is period L for the momentum $k \cong k + L$, we only need to consider the case with $1 \leq |k_{12}| \leq \frac{L}{2}$. There are $\frac{L(L+1)}{2}$ possible local states, and the probabilities are shown in Table 4.

local states	probabilities	ranges	numbers
$ j^2\rangle$	$p_{j^2} = \frac{2}{L^2}$	$j \in [1, L]$	L
$ j_1 j_2\rangle$	$p_{j_1 j_2} = \frac{4}{L^2} \cos^2 \frac{\pi j_{12} k_{12}}{L}$	$1 \leq j_1 < j_2 \leq L$	$\frac{L(L-1)}{2}$

Table 4: The local states and probabilities of the total system in the double-particle state $|k_1 k_2\rangle$ of the free bosonic chain.

For the subsystem A , there are $\frac{(\ell+1)(\ell+2)}{2}$ possible local states and the probabilities are shown in Table 5, where we have the marginal probabilities

$$p_{A,0} = \sum_{j=\ell+1}^L p_{j^2} + \sum_{\ell+1 \leq j_1 < j_2 \leq L} p_{j_1 j_2} = (1-x)^2 + \frac{\sin^2(\pi k_{12} x)}{L^2 \sin^2 \frac{\pi k_{12}}{L}}, \quad (\text{A.13})$$

$$p_{A,j} = \sum_{j_2=\ell+1}^L p_{j j_2} = \frac{2(1-x)}{L} - \frac{2 \sin(\pi k_{12} x) \cos \frac{2\pi k_{12}(j-\frac{\ell+1}{2})}{L}}{L^2 \sin \frac{\pi k_{12}}{L}}, \quad (\text{A.14})$$

with p_{j^2} and $p_{j_1 j_2}$ being defined in Table 4.

local states	probabilities	ranges	numbers
$ G\rangle_A$	$p_{A,0}$ (A.13)	-	1
$ j\rangle_A$	$p_{A,j}$ (A.14)	$j \in [1, \ell]$	ℓ
$ j^2\rangle_A$	$p_{A,j^2} = \frac{2}{L^2}$	$j \in [1, \ell]$	ℓ
$ j_1 j_2\rangle_A$	$p_{A,j_1 j_2} = \frac{4}{L^2} \cos^2 \frac{\pi j_{12} k_{12}}{L}$	$1 \leq j_1 < j_2 \leq \ell$	$\frac{\ell(\ell-1)}{2}$

Table 5: The local states and probabilities of the subsystem A in the double-particle state $|k_1 k_2\rangle$ of the free bosonic chain.

B States and probabilities in free fermionic chain

In this appendix, we show calculation details for the free fermionic chain.

B.1 Quasiparticle excited states

The free fermionic chain has the Hamiltonian

$$H = \sum_{j=1}^L \left(a_j^\dagger a_j - \frac{1}{2} \right). \quad (\text{B.1})$$

We define the global modes

$$b_k^\dagger \equiv \frac{1}{\sqrt{L}} \sum_{j=1}^L e^{\frac{2\pi i j k}{L}} a_j^\dagger, \quad b_k \equiv \frac{1}{\sqrt{L}} \sum_{j=1}^L e^{-\frac{2\pi i j k}{L}} a_j, \quad k = 0, 1, \dots, L-1. \quad (\text{B.2})$$

The ground state is defined as

$$a_j |G\rangle = b_k |G\rangle = 0, \quad \forall j, \forall k. \quad (\text{B.3})$$

Using the global modes b_k^\dagger , one could construct the general global state

$$|k_1 k_2 \dots k_s\rangle = b_{k_1}^\dagger b_{k_2}^\dagger \dots b_{k_s}^\dagger |G\rangle. \quad (\text{B.4})$$

Like the free bosonic chain, the natural local basis at each site is the eigenstates of the excitation number operator. One could also use the modes a_j^\dagger to construct the general locally excited state

$$|j_1 j_2 \dots j_s\rangle = a_{j_1}^\dagger a_{j_2}^\dagger \dots a_{j_s}^\dagger |G\rangle. \quad (\text{B.5})$$

In the Hilbert space of the subsystem $A = [1, \ell]$, one has similarly the subsystem ground state $|G\rangle_A$ defined as

$$a_j |G\rangle_A = 0, \quad \forall j \in A, \quad (\text{B.6})$$

as well as the subsystem local states

$$|j_1 j_2 \dots j_s\rangle_A = a_{j_1}^\dagger a_{j_2}^\dagger \dots a_{j_s}^\dagger |G\rangle_A, \quad j_1, j_2, \dots, j_s \in A. \quad (\text{B.7})$$

B.2 Single-particle state $|k\rangle$

The results for the single-particle state $|k\rangle$ in the free fermionic chain are the same as those in the free bosonic chain in appendix A.2. We will not repeat it here.

B.3 Double-particle state $|k_1 k_2\rangle$

We write the double-particle state $|k_1 k_2\rangle$ in terms of local states as

$$|k_1 k_2\rangle = \frac{2i}{L} \sum_{1 \leq j_1 < j_2 \leq L} e^{\frac{\pi i}{L}(j_1 + j_2)(k_1 + k_2)} \sin \frac{\pi j_{12} k_{12}}{L} |j_1 j_2\rangle, \quad (\text{B.8})$$

with $j_{12} = j_1 - j_2$ and $k_{12} = k_1 - k_2$. There are $\frac{L(L-1)}{2}$ possible local states $|j_1 j_2\rangle$ with $1 \leq j_1 < j_2 \leq L$, and the corresponding probabilities are

$$p_{j_1 j_2} = \frac{4}{L^2} \sin^2 \frac{\pi j_{12} k_{12}}{L}, \quad 1 \leq j_1 < j_2 \leq L. \quad (\text{B.9})$$

For the subsystem A , there are $\frac{\ell(\ell+1)}{2} + 1$ possible local states and the probabilities are shown in Table 6, where we have the marginal probabilities

$$p_{A,0} = \sum_{\ell+1 \leq j_1 < j_2 \leq L} p_{j_1 j_2} = (1-x)^2 - \frac{\sin^2(\pi k_{12} x)}{L^2 \sin^2 \frac{\pi k_{12}}{L}}, \quad (\text{B.10})$$

$$p_{A,j} = \sum_{j_2=\ell+1}^L p_{j_1 j_2} = \frac{2(1-x)}{L} + \frac{2 \sin(\pi k_{12} x) \cos \frac{2\pi k_{12}(j - \frac{\ell+1}{2})}{L}}{L^2 \sin \frac{\pi k_{12}}{L}}, \quad (\text{B.11})$$

with $p_{j_1 j_2}$ being defined in (B.9).

local states	probabilities	ranges	numbers
$ G\rangle_A$	$p_{A,0}$ (B.10)	-	1
$ j\rangle_A$	$p_{A,j}$ (B.11)	$j \in [1, \ell]$	ℓ
$ j_1 j_2\rangle_A$	$p_{A,j_1 j_2} = \frac{4}{L^2} \sin^2 \frac{\pi j_1 j_2 k_{12}}{L}$	$1 \leq j_1 < j_2 \leq \ell$	$\frac{\ell(\ell-1)}{2}$

Table 6: The local states and probabilities of the subsystem A in the double-particle state $|k_1 k_2\rangle$ of the free fermionic chain.

C States and probabilities in XXX chain

In this appendix, we show calculation details for the spin-1/2 XXX chain.

C.1 Magnon excited states

The spin-1/2 XXX chain has the Hamiltonian

$$H = -\frac{1}{4} \sum_{j=1}^L (\sigma_j^x \sigma_{j+1}^x + \sigma_j^y \sigma_{j+1}^y + \sigma_j^z \sigma_{j+1}^z) - \frac{h}{2} \sum_{j=1}^L \sigma_j^z, \quad (\text{C.1})$$

with a positive transverse field $h > 0$ and periodic boundary conditions for the Pauli matrices $\sigma_{L+1}^{x,y,z} = \sigma_1^{x,y,z}$. For simplicity, we also require that the number of sites L is four times of an integer. The unique ground state is

$$|G\rangle = |\uparrow\uparrow \cdots \uparrow\rangle. \quad (\text{C.2})$$

The low-lying eigenstates are magnon excited states in the ferromagnetic phase and can be obtained from the coordinate Bethe ansatz [63, 64]. One may use the Bethe numbers of the excited magnons $\{I_1, I_2, \cdots, I_s\}$ to denote magnon excited states as $|I_1 I_2 \cdots I_s\rangle$.

The presence of the transverse field in the Hamiltonian (C.1) makes the eigenstates of σ_j^z to be a natural local basis at each site for the XXX chain.² There are also local states, such as

$$|j\rangle = |\cdots \downarrow_j \cdots\rangle, \quad (\text{C.3})$$

in which only the site j has downward spin and all other sites have upward spins, and

$$|j_1 j_2\rangle = |\cdots \downarrow_{j_1} \cdots \downarrow_{j_2} \cdots\rangle, \quad (\text{C.4})$$

in which only the sites j_1, j_2 have downward spins and all other sites have upward spins. For the subsystem A , there are the subsystem local states $|G\rangle_A$ in which all the sites in A has upward spins, $|j\rangle_A$ in which only the site j in A has downward spin, and $|j_1 j_2\rangle_A$ in which only the sites j_1, j_2 in A have downward spins.

²In appendix G, we show the Shannon entropy in the local basis of σ_j^x eigenstates, and the results are very different from the those in σ_j^z basis.

C.2 Single-magnon state

The single magnon state takes the form

$$|I\rangle = \frac{1}{\sqrt{L}} \sum_{j=1}^L e^{\frac{2\pi i j I}{L}} |j\rangle, \quad (\text{C.5})$$

with the Bethe number $I = 0, 1, \dots, L-1$. The probability distributions are the same as those in the free bosonic chain in appendix A.2.

C.3 Double-magnon state

We consider the double-magnon state

$$|I_1 I_2\rangle = \frac{1}{\sqrt{\mathcal{N}}} \sum_{1 \leq j_1 < j_2 \leq L} \mathcal{U}_{j_1 j_2} |j_1 j_2\rangle, \quad (\text{C.6})$$

with the Bethe numbers I_1, I_2 which are integers and satisfy $0 \leq I_1 \leq I_2 \leq L-1$. There is

$$\mathcal{U}_{j_1 j_2} = e^{i(j_1 p_1 + j_2 p_2 + \frac{\theta}{2})} + e^{i(j_1 p_2 + j_2 p_1 - \frac{\theta}{2})}, \quad (\text{C.7})$$

with p_1, p_2, θ being solutions to the equation

$$e^{i\theta} = -\frac{1 + e^{i(p_1 + p_2)} - 2e^{ip_1}}{1 + e^{i(p_1 + p_2)} - 2e^{ip_2}}. \quad (\text{C.8})$$

The normalization factor is

$$\mathcal{N} = \sum_{1 \leq j_1 < j_2 \leq L} |\mathcal{U}_{j_1 j_2}|^2. \quad (\text{C.9})$$

In the state $|I_1 I_2\rangle$ there are two magnons with physical momenta p_1, p_2 and momenta k_1, k_2 related as

$$p_1 = \frac{2\pi k_1}{L}, \quad p_2 = \frac{2\pi k_2}{L}. \quad (\text{C.10})$$

To the equation (C.8), there are three cases of solutions, namely case I solution, case II solutions, and case III solutions. The case III solutions could be further classified into case IIIa solutions and case IIIb solutions.

C.3.1 Case I solution

For the case I solution, there are trivially

$$I_1 = p_1 = k_1 = I_2 = p_2 = k_2 = \theta = 0, \quad (\text{C.11})$$

and the state is

$$|00\rangle = \sqrt{\frac{2}{L(L-1)}} \sum_{1 \leq j_1 < j_2 \leq L} |j_1 j_2\rangle. \quad (\text{C.12})$$

The probability of the local state $|j_1 j_2\rangle$ is

$$p_{j_1 j_2}^I = \frac{2}{L(L-1)}, \quad 1 \leq j_1 < j_2 \leq L, \quad (\text{C.13})$$

which is the same as the probability distribution (E.11) in the configuration of two identical hard-core classical particles in subsection E.2.2.

C.3.2 Case II solution

For the case II solution $|I_1 I_2\rangle$, there are

$$k_1 = I_1 + \frac{\theta}{2\pi}, \quad k_2 = I_2 - \frac{\theta}{2\pi}, \quad (\text{C.14})$$

with Bethe numbers I_1, I_2 which satisfy $0 \leq I_1 < I_2 \leq L - 1$ and real shift angle $\theta \in [0, \pi]$. We have

$$k_{12} = I_{12} + \frac{\theta}{\pi}, \quad (\text{C.15})$$

with the momentum difference $k_{12} = k_1 - k_2$ and Bethe number difference $I_{12} = I_1 - I_2$. The normalization factor is

$$\mathcal{N} = L(L-1) + \frac{L \cos(\theta - p_{12}) - (L-1) \cos \theta - \cos(\theta - Lp_{12})}{1 - \cos p_{12}}. \quad (\text{C.16})$$

The probability that one finds the total system in the local state $|j_1 j_2\rangle$ is

$$p_{j_1 j_2}^{\text{II}} = \frac{2}{\mathcal{N}} [1 + \cos(j_{12} p_{12} + \theta)], \quad 1 \leq j_1 < j_2 \leq L, \quad (\text{C.17})$$

with $j_{12} = j_1 - j_2$ and $p_{12} = p_1 - p_2$. For the subsystem A , the probabilities of the subsystem local states $|G\rangle_A$, $|j\rangle_A$, and $|j_1 j_2\rangle_A$ are, respectively,

$$p_0^{A,\text{II}} = \frac{1}{\mathcal{N}} \left[(L-\ell)(L-\ell-1) + \frac{(L-\ell) \cos(p_{12} - \theta) - (L-\ell-1) \cos \theta - \cos[(L-\ell)p_{12} - \theta]}{1 - \cos p_{12}} \right], \quad (\text{C.18})$$

$$p_j^{A,\text{II}} = \frac{2}{\mathcal{N}} \left[L - \ell + \frac{\sin \frac{p_{12}(L-\ell)}{2} \cos[p_{12}(j - \frac{L+\ell+1}{2}) + \theta]}{\sin \frac{p_{12}}{2}} \right], \quad j \in [1, \ell], \quad (\text{C.19})$$

$$p_{j_1 j_2}^{A,\text{II}} = \frac{2}{\mathcal{N}} [1 + \cos(j_{12} p_{12} + \theta)], \quad 1 \leq j_1 < j_2 \leq \ell, \quad (\text{C.20})$$

which could be obtained as the marginal probabilities of (C.17).

C.3.3 Case IIIa solution

For the case IIIa solution, there are Bethe numbers

$$I_1 = \frac{I-1}{2}, \quad I_2 = \frac{I+1}{2}, \quad (\text{C.21})$$

with the total Bethe number

$$I = \tilde{I}, \tilde{I} + 2, \dots, \frac{L}{2} - 1, \frac{3L}{2} + 1, \frac{3L}{2} + 3, \dots, 2L - \tilde{I}, \quad (\text{C.22})$$

where \tilde{I} is an odd integer around $2\sqrt{L}/\pi$ in $L \rightarrow +\infty$ limit. Without loss of generality, we only need to consider $I = \tilde{I}, \tilde{I} + 2, \dots, \frac{L}{2} - 1$. The solution to the Bethe equation is

$$p_1 = \frac{\pi I}{L} + iv, \quad p_2 = \frac{\pi I}{L} - iv, \quad \theta = \pi + iLv. \quad (\text{C.23})$$

In $L \rightarrow +\infty$ limit, there is

$$v = -\log \left| \cos \frac{\pi I}{L} \right|, \quad (\text{C.24})$$

which is in the range

$$\frac{2}{L} \lesssim v \lesssim \log \frac{L}{\pi}. \quad (\text{C.25})$$

One could understand $1/v$ as the size of the bound state. The normalization factor is

$$\mathcal{N} = L \left[\frac{\sinh[(L-1)v]}{\sinh v} - (L-1) \right]. \quad (\text{C.26})$$

The probability that one finds the total system in the local state $|j_1 j_2\rangle$ is

$$p_{j_1 j_2}^{\text{IIIa}} = \frac{4}{\mathcal{N}} \sinh^2 \left[v \left(j_{12} + \frac{L}{2} \right) \right], \quad 1 \leq j_1 < j_2 \leq L, \quad (\text{C.27})$$

with $j_{12} = j_1 - j_2$. For the subsystem A , the probabilities of the subsystem local states $|G\rangle_A$, $|j\rangle_A$, and $|j_1 j_2\rangle_A$ are, respectively,

$$p_0^{A, \text{IIIa}} = \frac{1}{\mathcal{N}} \left[(L-\ell) \frac{\sinh[v(L-1)]}{\sinh v} - \frac{\sinh(v\ell) \sinh[v(L-\ell)]}{\sinh^2 v} - (L-\ell)(L-\ell-1) \right], \quad (\text{C.28})$$

$$p_j^{A, \text{IIIa}} = \frac{2}{\mathcal{N}} \left[\frac{\sinh[v(L-\ell)] \cosh[2v(j - \frac{\ell+1}{2})]}{\sinh v} - (L-\ell) \right], \quad j \in [1, \ell], \quad (\text{C.29})$$

$$p_{j_1 j_2}^{A, \text{IIIa}} = \frac{4}{\mathcal{N}} \sinh^2 \left[v \left(j_{12} + \frac{L}{2} \right) \right], \quad 1 \leq j_1 < j_2 \leq \ell, \quad (\text{C.30})$$

which are just the marginal probabilities of (C.27).

For finite v in the limit $L \rightarrow +\infty$, we have the probabilities

$$p_{j_1 j_2}^{\text{IIIa}} \rightarrow \frac{2 \sinh v}{L} e^{2v(|j_{12} + \frac{L}{2}| - \frac{L-1}{2})}, \quad 1 \leq j_1 < j_2 \leq L, \quad (\text{C.31})$$

and in the scaling limit there are

$$p_0^{\text{IIIa}} \rightarrow 1 - x, \quad (\text{C.32})$$

$$p_j^{\text{IIIa}} \rightarrow \frac{1}{L} e^{-2v(\frac{\ell-1}{2} - |j - \frac{\ell+1}{2}|)}, \quad j \in [1, \ell], \quad (\text{C.33})$$

$$p_{j_1 j_2}^{\text{IIIa}} \rightarrow \frac{2 \sinh v}{L} e^{-2v(\frac{L-1}{2} - |j_{12} + \frac{L}{2}|)}, \quad 1 \leq j_1 < j_2 \leq \ell. \quad (\text{C.34})$$

C.3.4 Case IIIb solution

For the case IIIb solution, there are Bethe numbers

$$I_1 = I_2 = \frac{I}{2}, \quad (\text{C.35})$$

with the total Bethe number

$$I = 2, 4, \dots, \frac{L}{2}, \frac{3L}{2}, \frac{3L}{2} + 2, \dots, 2L - 2. \quad (\text{C.36})$$

In the case with $I = \frac{L}{2}$, the state is extremely bound

$$|I_1 I_2\rangle = \frac{1}{\sqrt{L}} \sum_{j=1}^L e^{\frac{2\pi i I}{L}(j+\frac{1}{2})} |j, j+1\rangle, \quad (\text{C.37})$$

the results are the same as the those in the single-magnon state in subsection 4.1, and we will not repeat the calculations in this paper. Without loss of generality, we only consider $I = 2, 4, \dots, \frac{L}{2} - 2$. The solution to the equation (C.8) is

$$p_1 = \frac{\pi I}{L} + iv, \quad p_2 = \frac{\pi I}{L} - iv, \quad \theta = iLv. \quad (\text{C.38})$$

In $L \rightarrow +\infty$ limit, there is still

$$v = -\log \left| \cos \frac{\pi I}{L} \right|, \quad (\text{C.39})$$

which is in the range

$$\frac{2\pi^2}{L^2} \lesssim v \lesssim \log \frac{L}{\pi}. \quad (\text{C.40})$$

The normalization factor is

$$\mathcal{N} = L \left[\frac{\sinh[(L-1)v]}{\sinh v} + (L-1) \right]. \quad (\text{C.41})$$

The probability that one finds the total system in the local state $|j_1 j_2\rangle$ is

$$p_{j_1 j_2}^{\text{IIIb}} = \frac{4}{\mathcal{N}} \cosh^2 \left[v \left(j_{12} + \frac{L}{2} \right) \right], \quad 1 \leq j_1 < j_2 \leq L, \quad (\text{C.42})$$

with $j_{12} = j_1 - j_2$. For the subsystem A , the probabilities of the subsystem local states $|G\rangle_A$, $|j\rangle_A$, and $|j_1 j_2\rangle_A$ are, respectively,

$$p_0^{A, \text{IIIb}} = \frac{1}{\mathcal{N}} \left[(L-\ell) \frac{\sinh[v(L-1)]}{\sinh v} - \frac{\sinh(v\ell) \sinh[v(L-\ell)]}{\sinh^2 v} + (L-\ell)(L-\ell-1) \right], \quad (\text{C.43})$$

$$p_j^{A, \text{IIIb}} = \frac{2}{\mathcal{N}} \left[\frac{\sinh[v(L-\ell)] \cosh[2v(j - \frac{\ell+1}{2})]}{\sinh v} + (L-\ell) \right], \quad j \in [1, \ell], \quad (\text{C.44})$$

$$p_{j_1 j_2}^{A, \text{IIIb}} = \frac{4}{\mathcal{N}} \cosh^2 \left[v \left(j_{12} + \frac{L}{2} \right) \right], \quad 1 \leq j_1 < j_2 \leq \ell, \quad (\text{C.45})$$

which are the marginal probabilities of (C.42).

D SSH model

In this appendix, we consider the Su-Schrieffer-Heeger (SSH) model [57, 58] of a ring with L unit cells

$$H = \sum_{j=1}^L [v(a_{j,1}^\dagger a_{j,2} + a_{j,2}^\dagger a_{j,1}) + u(a_{j,2}^\dagger a_{j+1,1} + a_{j+1,1}^\dagger a_{j,2})], \quad (\text{D.1})$$

which describes electrons hopping on a dimerised lattice. In each unit cell labeled by $j = 1, 2, \dots, L$, there are fermionic modes $a_{j,\alpha}, a_{j,\alpha}^\dagger$ with $\alpha = 1, 2$. We only consider periodic boundary conditions. One could choose that the hopping constants v inside each unit cell and u between neighboring unit cells are nonnegative real numbers.

The SSH model could be diagonalized by the Fourier transformation

$$b_{k,\alpha}^\dagger = \frac{1}{\sqrt{L}} \sum_{j=1}^L e^{\frac{2\pi i j k}{L}} a_{j,\alpha}^\dagger, \quad b_{k,\alpha} = \frac{1}{\sqrt{L}} \sum_{j=1}^L e^{-\frac{2\pi i j k}{L}} a_{j,\alpha},$$

$$k = 0, 1, \dots, L-1, \quad \alpha = 1, 2. \quad (\text{D.2})$$

followed by the transformation

$$c_{k,\pm}^\dagger = \frac{1}{\sqrt{2}} (b_{k,1}^\dagger \pm e^{i\theta_k} b_{k,2}^\dagger), \quad c_{k,\pm} = \frac{1}{\sqrt{2}} (b_{k,1} \pm e^{-i\theta_k} b_{k,2}), \quad (\text{D.3})$$

where the angle θ_k is determined by

$$e^{i\theta_k} = \frac{v + u e^{\frac{2\pi i k}{L}}}{\varepsilon_k}, \quad \varepsilon_k = \sqrt{v^2 + u^2 + 2vu \cos \frac{2\pi k}{L}}. \quad (\text{D.4})$$

The Hamiltonian becomes that of the double copies of the free fermionic chains

$$H = \sum_k \varepsilon_k (c_{k,+}^\dagger c_{k,+} - c_{k,-}^\dagger c_{k,-}). \quad (\text{D.5})$$

In the SSH model there are two sets of independent fermionic modes, namely the modes $c_{k,+}, c_{k,+}^\dagger$ and the modes $c_{k,-}, c_{k,-}^\dagger$. One may define the empty state $|\emptyset\rangle$ as

$$c_{k,\pm}|\emptyset\rangle = 0, \quad k = 0, 1, \dots, L-1, \quad (\text{D.6})$$

based on which a general excited states $|K_+, K_-\rangle$ with modes $K_+ = \{k_1^+, k_2^+, \dots, k_{r_+}^+\}$ and $K_- = \{k_1^-, k_1^-, \dots, k_{r_-}^-\}$ may be constructed as

$$|K_+, K_-\rangle = c_{k_1^+,+}^\dagger c_{k_2^+,+}^\dagger \cdots c_{k_{r_+}^+,+}^\dagger c_{k_1^-,-}^\dagger c_{k_2^-,-}^\dagger \cdots c_{k_{r_-}^-,-}^\dagger |\emptyset\rangle. \quad (\text{D.7})$$

As the modes K_+ and K_- are independent, their contributions to the entanglement entropy and Shannon entropy are also independent. Then we have the entanglement entropy in the SSH model as the sum of the entanglement entropies in the free fermionic chain

$$S_{A,\{K_+,K_-\}}^{\text{SSH}} = S_{A,K_+}^{\text{fer}} + S_{A,K_-}^{\text{fer}}. \quad (\text{D.8})$$

There are similar results for the Shannon entropy and mutual information

$$\begin{aligned} H_{\{K_+,K_-\}}^{\text{SSH}}(L) &= H_{A,K_+}^{\text{fer}}(L) + H_{A,K_-}^{\text{fer}}(L), \\ H_{\{K_+,K_-\}}^{\text{SSH}}(\ell) &= H_{A,K_+}^{\text{fer}}(\ell) + H_{A,K_-}^{\text{fer}}(\ell), \\ M_{\{K_+,K_-\}}^{\text{SSH}}(\ell) &= M_{A,K_+}^{\text{fer}}(\ell) + M_{A,K_-}^{\text{fer}}(\ell). \end{aligned} \quad (\text{D.9})$$

E Classical particles

This appendix presents the calculation of the Shannon entropy and mutual information for classical particle configurations on a circular chain. Both soft-core and hard-core particles are considered, corresponding to the classical limits of bosonic and fermionic quantum particles, respectively.

E.1 Soft-core classical particles

We start with soft-core classical particles, which can have any number of particles at one site, i.e. a site can be empty, occupied by one particle, or occupied by more than one particle.

E.1.1 One particle

We consider the macroscopic configuration of the chain in which there is one soft-core classical particle. There are L possible microscopic configurations, i.e. the particle at site j with $j \in [1, L]$, and probabilities are

$$p_j = \frac{1}{L}, \quad j \in [1, L]. \quad (\text{E.1})$$

The Shannon entropy of the whole system is

$$H_1^{\text{soft}}(L) = \log L. \quad (\text{E.2})$$

For the subsystem A , there are $\ell + 1$ possible microscopic configurations, as shown in Table 7. The Shannon entropy of the subsystem A is

$$H_1^{\text{soft}}(\ell) = x \log L - (1 - x) \log(1 - x). \quad (\text{E.3})$$

The Shannon mutual information is

$$M_1^{\text{soft}}(\ell) = -x \log x - (1 - x) \log(1 - x), \quad (\text{E.4})$$

which is just the Shannon entropy of the probability distribution of the coarse-grained subsystem configurations $\{x, 1 - x\}$. Observe that the values of $1 - x$ and x correspond to the presence of no particle and one particle, respectively, in the subsystem A .

microscopic configurations	probabilities	ranges	numbers
no particle in A	$p_{A,0} = 1 - x$	-	1
one particle in A at j	$p_{A,j} = \frac{1}{L}$	$j \in [1, \ell]$	ℓ

Table 7: The microscopic configurations and probabilities of the subsystem A in the macroscopic configuration of one soft-core classical particle.

E.1.2 Two identical particles

We consider the macroscopic configuration in which there are two identical particles on the chain. For the total system, there are $\frac{L(L+1)}{2}$ possible microscopic configurations as shown in Table 8. In the scaling limit, the Shannon entropy of the total system is

$$H_{1^2}^{\text{soft}}(L) = 2 \log L - \log 2. \quad (\text{E.5})$$

microscopic configurations	probabilities	ranges	numbers
both at j	$p_{j^2} = \frac{1}{L^2}$	$j \in [1, L]$	L
one at j_1 and the other at j_2	$p_{j_1 j_2} = \frac{2}{L^2}$	$1 \leq j_1 < j_2 \leq L$	$\frac{L(L-1)}{2}$

Table 8: The microscopic configurations and probabilities of the total system in the macroscopic configuration of two identical soft-core classical particles.

For the subsystem A , there are $\frac{(\ell+1)(\ell+2)}{2}$ different microscopic configurations, as shown in Table 9. In the scaling limit, we get the Shannon entropy of the subsystem A

$$H_{1^2}^{\text{soft}}(\ell) = 2x \log L - x(2 - x) \log 2 - 2(1 - x) \log(1 - x). \quad (\text{E.6})$$

In the scaling limit, the mutual information is

$$\begin{aligned} M_{1^2}^{\text{soft}}(\ell) &= -x^2 \log x^2 - 2x(1 - x) \log[2x(1 - x)] - (1 - x)^2 \log(1 - x)^2 \\ &= -2x \log x - 2(1 - x) \log(1 - x) - 2x(1 - x) \log 2, \end{aligned} \quad (\text{E.7})$$

which is just the Shannon entropy of the probability distribution of the coarse-grained subsystem configurations $\{x^2, 2x(1 - x), (1 - x)^2\}$.

microscopic configurations	probabilities	ranges	numbers
no particle in A	$p_{A,0} = (1-x)^2$	-	1
only one particle in A at j	$p_{A,j} = \frac{2(1-x)}{L}$	$j \in [1, \ell]$	ℓ
both in A at j	$p_{A,j^2} = \frac{1}{L^2}$	$j \in [1, \ell]$	ℓ
both in A with one at j_1 and the other at j_2	$p_{A,j_1 j_2} = \frac{2}{L^2}$	$1 \leq j_1 < j_2 \leq \ell$	$\frac{\ell(\ell-1)}{2}$

Table 9: The microscopic configurations and probabilities of the subsystem A in the macroscopic configuration of two identical soft-core classical particles.

E.1.3 Two distinguishable particle

We consider two distinguishable particles, say one red particle and one blue particle. There are L^2 possible microscopic configurations, as shown in Table 10. The Shannon entropy is

$$H_{12}^{\text{soft}}(L) = 2 \log L. \quad (\text{E.8})$$

microscopic configurations	probabilities	ranges	numbers
both at j	$p_{j^2} = \frac{1}{L^2}$	$j \in [1, L]$	L
red at j_1 with blue at j_2	$p_{j_1 j_2} = \frac{1}{L^2}$	$j_1, j_2 \in [1, L], j_1 \neq j_2$	$L(L-1)$

Table 10: The microscopic configurations and probabilities of the total system in the macroscopic configuration of two distinguishable soft-core classical particles.

For the subsystem A , there are $(\ell+1)(\ell+2)$ possible configurations, as shown in Table 11. We get the Shannon entropy of the subsystem

$$H_{12}^{\text{soft}}(\ell) = 2x \log L - 2(1-x) \log(1-x). \quad (\text{E.9})$$

The mutual information is

$$M_{12}^{\text{soft}}(\ell) = 2[-x \log x - (1-x) \log(1-x)], \quad (\text{E.10})$$

which is just the Shannon entropy of the probability distribution of the coarse-grained subsystem configurations $\{x, 1-x\} \otimes \{x, 1-x\} = \{x^2, x(1-x), x(1-x), (1-x)^2\}$.

E.2 Hard-core classical particles

We next consider classical particles with the restriction that a site can have only one particle at most.

E.2.1 One particle

This case of one hard-core classical particle is identical to that of one soft-core classical particle in subsection E.1.1. We will skip it here.

microscopic configurations	probabilities	ranges	numbers
no particle in A	$p_{A,0} = (1-x)^2$	-	1
only red particle in A at j	$p_{A,j}^{\text{red}} = \frac{1-x}{L}$	$j \in [1, \ell]$	ℓ
only blue particle in A at j	$p_{A,j}^{\text{blue}} = \frac{1-x}{L}$	$j \in [1, \ell]$	ℓ
both in A at j	$p_{A,j^2} = \frac{1}{L^2}$	$j = 1, 2, \dots, L$	ℓ
both in A with red at j_1 and blue at j_2	$p_{A,j_1 j_2} = \frac{1}{L^2}$	$j_1, j_2 \in [1, \ell], j_1 \neq j_2$	$\ell(\ell-1)$

Table 11: The microscopic configurations and probabilities of the subsystem A in the macroscopic configuration of two distinguishable soft-core classical particles.

E.2.2 Two identical particles

We consider two identical hard-core classical particles. There are $\frac{L(L-1)}{2}$ possible microscopic configurations, i.e. that one particle at site j_1 and the other particle at site j_2 with $1 \leq j_1 < j_2 \leq L$, and the corresponding probabilities are

$$p_{j_1 j_2} = \frac{2}{L(L-1)}, \quad 1 \leq j_1 < j_2 \leq L. \quad (\text{E.11})$$

In the scaling limit, the Shannon entropy of the total system is

$$H_{1^2}^{\text{hard}}(L) = 2 \log L - \log 2. \quad (\text{E.12})$$

For the subsystem A , there are $\frac{\ell(\ell+1)}{2} + 1$ possible configurations, as shown in Table 12. In the scaling limit, we get the Shannon entropy of the subsystem

$$H_{1^2}^{\text{hard}}(\ell) = 2x \log L - 2(1-x) \log(1-x) - x(2-x) \log 2. \quad (\text{E.13})$$

In the scaling limit, the mutual information is

$$\begin{aligned} M_{1^2}^{\text{hard}}(\ell) &= -2x \log x - 2(1-x) \log(1-x) - 2x(1-x) \log 2 \\ &= -x^2 \log x^2 - 2x(1-x) \log[2x(1-x)] - (1-x)^2 \log(1-x)^2, \end{aligned} \quad (\text{E.14})$$

which is just the Shannon entropy of the probability distribution $\{x^2, 2x(1-x), (1-x)^2\}$. In the scaling limit, the results in this subsection are the same as those in subsection E.1.2.

microscopic configurations	probabilities	ranges	numbers
no particle in A	$p_{A,0} = \frac{(L-\ell)(L-\ell-1)}{L(L-1)}$	-	1
only one particle in A at j	$p_{A,j} = \frac{2(L-\ell)}{L(L-1)}$	$j \in [1, \ell]$	ℓ
both in A with at j_1, j_2	$p_{A,j_1 j_2} = \frac{2}{L(L-1)}$	$1 \leq j_1 < j_2 \leq \ell$	$\frac{\ell(\ell-1)}{2}$

Table 12: The microscopic configurations and probabilities of the subsystem A in the macroscopic configuration of two identical hard-core classical particles.

E.2.3 Two distinguishable particles

We consider two distinguishable particles, say one red particle and one blue particle. There are $L(L-1)$ possible microscopic configurations, i.e. that the red particle at site j_1 and the blue particle at site j_2 with $j_1, j_2 \in [1, L]$ and $j_1 \neq j_2$, and the corresponding probabilities are

$$p_{j_1 j_2} = \frac{1}{L(L-1)}, \quad j_1, j_2 \in [1, L], \quad j_1 \neq j_2. \quad (\text{E.15})$$

In the scaling limit, the Shannon entropy is

$$H_{12}^{\text{hard}}(L) = 2 \log L. \quad (\text{E.16})$$

For the subsystem A , there are $\ell^2 + \ell + 1$ possible configurations, as shown in Table 13. In the scaling limit, we get the Shannon entropy of the subsystem

$$H_{12}^{\text{hard}}(\ell) = 2x \log L - 2(1-x) \log(1-x). \quad (\text{E.17})$$

In the scaling limit, the mutual information is

$$M_{12}^{\text{hard}}(\ell) = 2[-x \log x - (1-x) \log(1-x)], \quad (\text{E.18})$$

which is just the Shannon entropy of the probability distribution $\{x, 1-x\} \otimes \{x, 1-x\} = \{x^2, x(1-x), x(1-x), (1-x)^2\}$. In the scaling limit, the results in this subsection are the same as those in subsection E.1.3.

microscopic configurations	probabilities	ranges	numbers
no particle in A	$p_{A,0} = \frac{(L-\ell)(L-\ell-1)}{L(L-1)}$	-	1
only red particle in A at j	$p_{A,j}^{\text{red}} = \frac{L-\ell}{L(L-1)}$	$j \in [1, \ell]$	ℓ
only blue particle in A at j	$p_{A,j}^{\text{blue}} = \frac{L-\ell}{L(L-1)}$	$j \in [1, \ell]$	ℓ
both in A with red at j_1 and blue at j_2	$p_{A,j_1 j_2} = \frac{1}{L(L-1)}$	$j_1, j_2 \in [1, \ell], j_1 \neq j_2$	$\ell(\ell-1)$

Table 13: The microscopic configurations and probabilities of the subsystem A in the macroscopic configuration of two distinguishable hard-core classical particles.

E.3 Summary and generalization

When the number of particles is finite, the Shannon entropy and mutual information in the scaling limit only depend on the number of particles and how distinguishable they are, not on the limit of the number of particles at each site. This means that we get the same results for soft-core and hard-core classical particles in the scaling limit. Moreover, the Shannon mutual information is equal to the Shannon entropy of the probability distribution of the coarse-grained subsystem configurations.

We summarize the results in this appendix as follows. For the macroscopic configuration of one classical particle, in the scaling limit we get the total system Shannon entropy, subsystem Shannon

entropy and mutual information

$$H_1^{\text{cl}}(L) = \log L, \quad (\text{E.19})$$

$$H_1^{\text{cl}}(\ell) = x \log L - (1-x) \log(1-x), \quad (\text{E.20})$$

$$M_1^{\text{cl}}(\ell) = -x \log x - (1-x) \log(1-x). \quad (\text{E.21})$$

For two identical classical particles, we get

$$H_{12}^{\text{cl}}(L) = 2 \log L - \log 2, \quad (\text{E.22})$$

$$H_{12}^{\text{cl}}(\ell) = 2x \log L - 2(1-x) \log(1-x) - x(2-x) \log 2, \quad (\text{E.23})$$

$$M_{12}^{\text{cl}}(\ell) = -x^2 \log x^2 - 2x(1-x) \log[2x(1-x)] - (1-x)^2 \log(1-x)^2. \quad (\text{E.24})$$

For two distinguishable classical particles, we get

$$H_{12}^{\text{cl}}(L) = 2 \log L, \quad (\text{E.25})$$

$$H_{12}^{\text{cl}}(\ell) = 2x \log L - 2(1-x) \log(1-x), \quad (\text{E.26})$$

$$M_{12}^{\text{cl}}(\ell) = -2x \log x - 2(1-x) \log(1-x). \quad (\text{E.27})$$

For more general cases, we just show the final results without giving any calculation details. For r identical particles with finite r in the scaling limit $L \rightarrow +\infty$, $\ell \rightarrow +\infty$, and fixed $x = \ell/L$, we obtain

$$H_{1r}^{\text{cl}}(L) = r \log L - \log r!, \quad (\text{E.28})$$

$$H_{1r}^{\text{cl}}(\ell) = rx \log L - \sum_{i=0}^r C_r^i x^i (1-x)^{r-i} \log[i! C_r^i (1-x)^{r-i}], \quad (\text{E.29})$$

$$M_{1r}^{\text{cl}}(\ell) = - \sum_{i=0}^r C_r^i x^i (1-x)^{r-i} \log[C_r^i x^i (1-x)^{r-i}], \quad (\text{E.30})$$

with the binomial coefficient $C_r^i \equiv \frac{r!}{i!(r-i)!}$. For s different kinds of particles with the number of the i -th kind of particles being r_i , $i = 1, 2, \dots, s$ and total number of particles $R = \sum_{i=1}^s r_i$ being finite in the scaling limit, we get

$$H_{1r_1 2r_2 \dots s r_s}^{\text{cl}}(L) = \sum_{i=1}^s H_{1r_i}^{\text{cl}}(L), \quad (\text{E.31})$$

$$H_{1r_1 2r_2 \dots s r_s}^{\text{cl}}(\ell) = \sum_{i=1}^s H_{1r_i}^{\text{cl}}(\ell), \quad (\text{E.32})$$

$$M_{1r_1 2r_2 \dots s r_s}^{\text{cl}}(\ell) = \sum_{i=1}^s M_{1r_i}^{\text{cl}}(\ell). \quad (\text{E.33})$$

In the scaling limit, the contributions of different classical particles to the total system Shannon entropy, subsystem Shannon entropy and mutual information become independent. However, the Shannon entropy and mutual information of quantum quasiparticles do not exhibit such decoupling property even in the limit of large momentum difference, as shown in the main text of the paper.

F Shannon entropy of particle number probability distribution

In this section, we determine the Shannon entropy for the probability distribution of subsystem particle numbers in free bosonic and fermionic chains, which are just the number entropy studied in for example [15, 65, 66]. The semiclassical quasiparticle picture applies to the Shannon entropy of particle number probability distribution in the large momentum difference limit.

F.1 Classical particles

For finite number of classical particles in the scaling limit, the subsystem Shannon entropy of particle number probability distribution only depends on the total number of particles R , regardless the distinguishability of these particles. The result is also not dependent on the limit of the particle number at one site. In the limit $R \ll \ell < L$, the result is just the Shannon entropy of a binomial probability distribution

$$H_R^{\text{cl}}(\ell) = - \sum_{r=0}^R C_R^r x^r (1-x)^{R-r} \log[C_R^r x^r (1-x)^{R-r}], \quad (\text{F.1})$$

with the binomial coefficient $C_R^r = \frac{R!}{r!(R-r)!}$.

F.2 Free bosonic chain

In the single-particle state $|k\rangle$ and double-particle state $|k^2\rangle$ of the free bosonic chain, the results are trivial and the same as those of classical particles. We skip the calculations here.

In the double-particle state $|k_1 k_2\rangle$, the probabilities of finding zero, one, and two particles in the subsystem $A = [1, \ell]$ are respectively

$$p_{A,0}^{\text{bos}} = p_{A,0} = (1-x)^2 + \frac{\sin^2(\pi k_{12} x)}{L^2 \sin^2 \frac{\pi k_{12}}{L}}, \quad (\text{F.2})$$

$$p_{A,1}^{\text{bos}} = \sum_{j=1}^{\ell} p_{A,j} = 2 \left[x(1-x) - \frac{\sin^2(\pi k_{12} x)}{L^2 \sin^2 \frac{\pi k_{12}}{L}} \right], \quad (\text{F.3})$$

$$p_{A,2}^{\text{bos}} = \sum_{j=1}^{\ell} p_{A,j^2} + \sum_{1 \leq j_1 < j_2 \leq \ell} p_{A,j_1 j_2} = x^2 + \frac{\sin^2(\pi k_{12} x)}{L^2 \sin^2 \frac{\pi k_{12}}{L}}, \quad (\text{F.4})$$

with $p_{A,0}$, $p_{A,j}$, p_{A,j^2} and $p_{A,j_1 j_2}$ being defined in Table 5. The corresponding Shannon entropy is just

$$H_{k_1 k_2}^{\text{bos}}(\ell) = -p_{A,0}^{\text{bos}} \log p_{A,0}^{\text{bos}} - p_{A,1}^{\text{bos}} \log p_{A,1}^{\text{bos}} - p_{A,2}^{\text{bos}} \log p_{A,2}^{\text{bos}}. \quad (\text{F.5})$$

In the large momentum difference limit $|k_{12}| \gg 1$, the result approaches that of two classical particles

$$\lim_{|k_{12}| \rightarrow +\infty} H_{k_1 k_2}^{\text{bos}}(\ell) = H_2^{\text{cl}}(\ell). \quad (\text{F.6})$$

F.3 Free fermionic chain

In the double-particle state $|k_1 k_2\rangle$ of the free fermionic chain, the probability of finding zero, one, and two particles in the subsystem $A = [1, \ell]$ are respectively

$$p_{A,0}^{\text{fer}} = p_{A,0} = (1-x)^2 - \frac{\sin^2(\pi k_{12} x)}{L^2 \sin^2 \frac{\pi k_{12}}{L}}, \quad (\text{F.7})$$

$$p_{A,1}^{\text{fer}} = \sum_{j=1}^{\ell} p_{A,j} = 2 \left[x(1-x) + \frac{\sin^2(\pi k_{12} x)}{L^2 \sin^2 \frac{\pi k_{12}}{L}} \right], \quad (\text{F.8})$$

$$p_{A,2}^{\text{fer}} = \sum_{1 \leq j_1 < j_2 \leq \ell} p_{A,j_1 j_2} = x^2 - \frac{\sin^2(\pi k_{12} x)}{L^2 \sin^2 \frac{\pi k_{12}}{L}}. \quad (\text{F.9})$$

with $p_{A,0}$, $p_{A,j}$ and $p_{A,j_1 j_2}$ being defined in Table 6. The corresponding Shannon entropy is

$$H_{k_1 k_2}^{\text{fer}}(\ell) = -p_{A,0}^{\text{fer}} \log p_{A,0}^{\text{fer}} - p_{A,1}^{\text{fer}} \log p_{A,1}^{\text{fer}} - p_{A,2}^{\text{fer}} \log p_{A,2}^{\text{fer}}, \quad (\text{F.10})$$

and in the large momentum difference limit $|k_{12}| \gg 1$ it also approaches that of two classical particles

$$\lim_{|k_{12}| \rightarrow +\infty} H_{k_1 k_2}^{\text{fer}}(\ell) = H_2^{\text{cl}}(\ell). \quad (\text{F.11})$$

G Shannon entropy in σ_j^x basis of XXX chain

This appendix focuses on the investigation of the Shannon entropy in the local basis of eigenstates of σ_j^x for the XXX chain.³

G.1 The σ_j^x basis

For a single set of Pauli matrices $\{\sigma^x, \sigma^y, \sigma^z\}$, the eigenstates of σ^x is

$$|\pm\rangle = \frac{1}{\sqrt{2}}(|\uparrow\rangle \pm |\downarrow\rangle). \quad (\text{G.1})$$

In the local basis of σ_j^x eigenstates, there are local states which we denote as $|\mathcal{X}\rangle$ with \mathcal{X} being a set of numbers in the range $[1, L]$. In the state $|\mathcal{X}\rangle$, the site $j \notin \mathcal{X}$ has spin $|+\rangle$ and the site $j \in \mathcal{X}$ has spin $|-\rangle$. For example, in this appendix we use the local states

$$\begin{aligned} |\emptyset\rangle &= |++\cdots+\rangle, \\ |j\rangle &= |\cdots -_j \cdots\rangle, \\ |j_1 j_2\rangle &= |\cdots -_{j_1} \cdots -_{j_2} \cdots\rangle, \end{aligned} \quad (\text{G.2})$$

where all the omitted sites have spin $|+\rangle$. For the total system with L sites, there are 2^L states $\{|\mathcal{X}\rangle\}$ in σ_j^x basis. For the subsystem $A = [1, \ell]$, there are similarly 2^ℓ states $\{|\mathcal{X}\rangle_A\}$.

³We thank M. A. Rajabpour for suggesting us to look into the case of Shannon entropy in the σ_j^x local basis.

G.2 Ground state

In the ground state of the ferromagnetic XXX chain $|G\rangle = |\uparrow\uparrow \cdots \uparrow\rangle$, the probability of the local state $|\mathcal{X}\rangle$ is

$$p_{\mathcal{X}}^G = \frac{1}{2^L}, \quad (\text{G.3})$$

from which we get the Shannon entropy of the total system

$$H_G^{\text{XXX}}(L) = L \log 2. \quad (\text{G.4})$$

Similarly, we get the probability of the local state $|\mathcal{X}\rangle_A$

$$p_{\mathcal{X}}^{A,G} = \frac{1}{2^\ell}, \quad (\text{G.5})$$

and the subsystem Shannon entropy

$$H_G^{\text{XXX}}(\ell) = \ell \log 2. \quad (\text{G.6})$$

Note that the total system and subsystem Shannon entropies take the maximal values. The subsystem Shannon mutual information is trivial

$$M_G^{\text{XXX}}(\ell) = 0. \quad (\text{G.7})$$

G.3 Single-magnon state

In the single-magnon state

$$|I\rangle = \frac{1}{\sqrt{L}} \sum_{j=1}^L e^{\frac{2\pi i j I}{L}} |j\rangle, \quad I = 0, 1, \dots, L-1, \quad (\text{G.8})$$

the probability of the local state $|\mathcal{X}\rangle$ of the total system is

$$p_{\mathcal{X}}^I = \frac{1}{2^L L} \left| \sum_{j=1}^L e^{\frac{2\pi i j I}{L}} m_{j,\mathcal{X}} \right|^2, \quad (\text{G.9})$$

with $m_{j,\mathcal{X}} = 1$ for $j \notin \mathcal{X}$ and $m_{j,\mathcal{X}} = -1$ for $j \in \mathcal{X}$. The total system Shannon entropy could be evaluated numerically as

$$H_I^{\text{XXX}}(L) = - \sum_{\mathcal{X}} p_{\mathcal{X}}^I \log p_{\mathcal{X}}^I. \quad (\text{G.10})$$

Similarly, the probability of the subsystem local state $|\mathcal{X}\rangle_A$ is

$$p_{\mathcal{X}}^{A,I} = \frac{1}{2^\ell} \left(1 - \frac{\ell}{L} + \frac{1}{L} \left| \sum_{j=1}^{\ell} e^{\frac{2\pi i j I}{L}} m_{j,\mathcal{X}} \right|^2 \right), \quad (\text{G.11})$$

from which we calculate the subsystem Shannon entropy as

$$H_I^{\text{XXX}}(\ell) = - \sum_{\mathcal{X}} p_{\mathcal{X}}^{A,I} \log p_{\mathcal{X}}^{A,I}. \quad (\text{G.12})$$

The subsystem Shannon mutual information is

$$M_I^{\text{XXX}}(\ell) = H_I^{\text{XXX}}(\ell) + H_I^{\text{XXX}}(L - \ell) - H_I^{\text{XXX}}(L). \quad (\text{G.13})$$

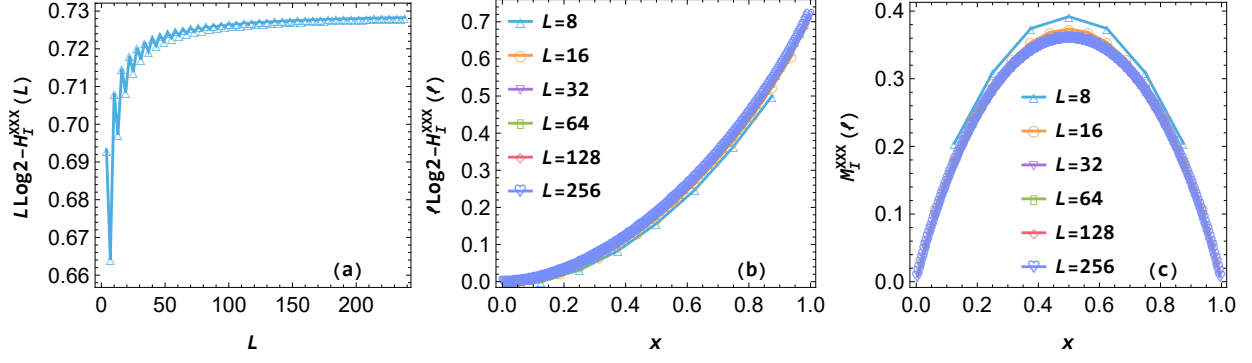


Figure 15: The σ_j^x basis total system and subsystem Shannon entropies and mutual information in the single-magnon state of the XXX chain with Bethe numbers $I = 0$ and $I = L/2$.

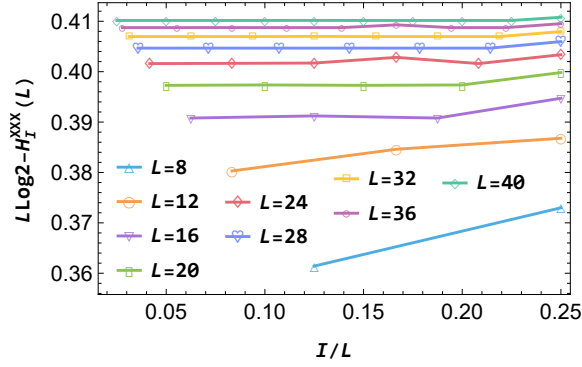


Figure 16: The σ_j^x basis total system Shannon entropy $H_I^{\text{XXX}}(L)$ (G.10) in the single-magnon state of the XXX chain for $I \in [1, L/4]$.

For the special cases $I = 0$ and $I = L/2$, the formulas of the Shannon entropies $H_I^{\text{XXX}}(L)$ (G.10) and $H_I^{\text{XXX}}(\ell)$ (G.12) could be further simplified, and we obtain

$$H_0^{\text{XXX}}(L) = H_{L/2}^{\text{XXX}}(L) = L \log 2 - \frac{1}{2L} \sum_{n=0}^L C_L^n \left(L - 4n + \frac{4n^2}{L} \right) \log \left(L - 4n + \frac{4n^2}{L} \right), \quad (\text{G.14})$$

$$M_0^{\text{XXX}}(L) = M_{L/2}^{\text{XXX}}(L) = \ell \log 2 - \frac{1}{2^\ell} \sum_{n=0}^{\ell} C_\ell^n \left(1 + \frac{\ell^2 - (4n+1)\ell + 4n^2}{L} \right) \log \left(1 + \frac{\ell^2 - (4n+1)\ell + 4n^2}{L} \right). \quad (\text{G.15})$$

We show the special results of the total system and subsystem Shannon entropies and mutual information with $I = 0$ and $I = L/2$ in Figure 15. From the left panel we see that in large L limit there are

$$H_0^{\text{XXX}}(L) = H_{L/2}^{\text{XXX}}(L) = L \log 2 - C_0 = L \log 2 - C_{L/2}, \quad (\text{G.16})$$

with the L -independent constant $C_0 = C_{L/2} \approx 0.73$. From the middle and right panels, we see that in the scaling limit there are

$$H_0^{\text{XXX}}(\ell) = \ell \log 2 - F_0(x) = H_{L/2}^{\text{XXX}}(\ell) = \ell \log 2 - F_{L/2}(x), \quad (\text{G.17})$$

$$M_0^{\text{XXX}}(\ell) = G_0(x) = M_{L/2}^{\text{XXX}}(\ell) = G_{L/2}(x), \quad (\text{G.18})$$

with the finite functions $F_0(x) = F_{L/2}(x)$ and $G_0(x) = G_{L/2}(x)$ depending on the ratio $x = \ell/L$.

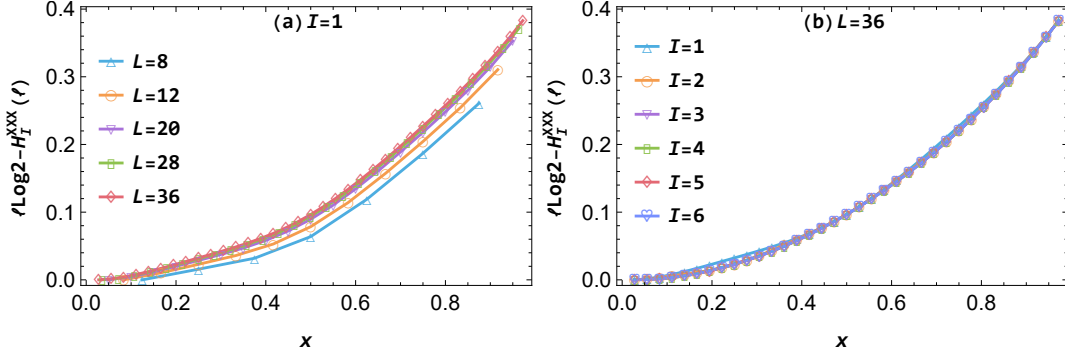


Figure 17: The σ_j^x basis subsystem Shannon entropy $H_I^{\text{XXX}}(\ell)$ (G.12) in the single-magnon state of the XXX chain.

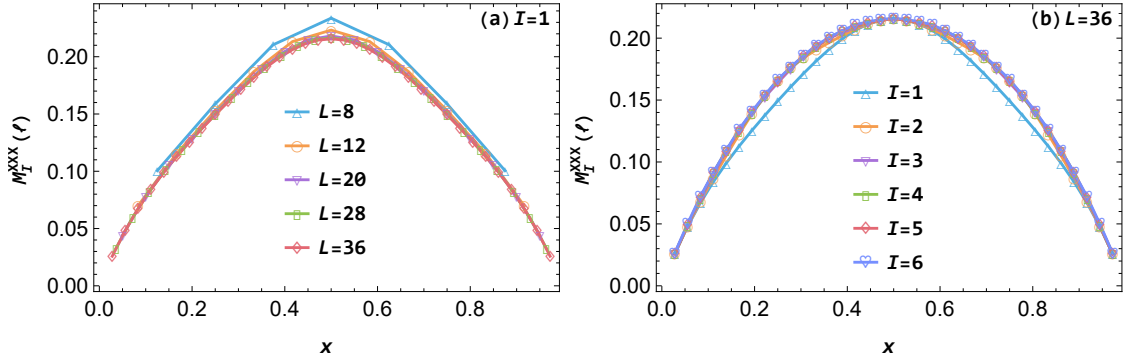


Figure 18: The σ_j^x basis subsystem Shannon mutual information $M_I^{\text{XXX}}(\ell)$ (G.13) in the single-magnon state of the XXX chain.

For general I , the evaluations of the σ_j^x basis total system Shannon entropy and the subsystem Shannon entropy and mutual information are exponentially difficult problems, and we could only numerically calculate them for not so large L , say $L \leq 36$. It is easy to see that both the total system and subsystem Shannon entropies $H_I^{\text{XXX}}(L)$ (G.10) and $H_I^{\text{XXX}}(\ell)$ (G.12) are invariant under the changes $I \rightarrow L - I$ and $I \rightarrow \frac{L}{2} - I$, and so without loss of generality we only need to consider I in the range $[1, L/4]$. We show the numerical results of $H_I^{\text{XXX}}(L)$ (G.10), $H_I^{\text{XXX}}(\ell)$ (G.12), and $M_I^{\text{XXX}}(\ell)$ (G.13) in, respectively figures 16, 17 and 18. From Figure 16, we see that in large L limit the total system Shannon entropy takes the form

$$H_I^{\text{XXX}}(L) = L \log 2 - C_I, \quad (\text{G.19})$$

with C_I being a constant that depends on the relative values of I and L . We anticipate that for most values of I there is the universal constant $C_I \approx 0.41$, and for a few exception values of I the constant C_I may take some exceptional values, like the cases $I = 0$ and $I = L/2$ discussed above. From Figure 17, in the scaling limit the subsystem Shannon entropy takes the form

$$H_I^{\text{XXX}}(\ell) = \ell \log 2 - F_I(x), \quad (\text{G.20})$$

with the I -dependence function $F_I(x)$. From Figure 18, in the scaling limit the subsystem Shannon mutual information takes the form

$$M_I^{\text{XXX}}(\ell) = G_I(x), \quad (\text{G.21})$$

with the I -dependence function $G_I(x)$. We expect that in the scaling limit, for $I \gg 1$ with a few possible exceptional values excluded, the functions $F_I(x)$ and $G_I(x)$ will take on respective universal forms.

References

- [1] L. Venema, B. Verberck, I. Georgescu, G. Prando, E. Couderc, S. Milana, M. Maragkou, L. Persechini, G. Pacchioni and L. Fleet, *The quasiparticle zoo*, [Nat. Phys. **12**, 1085–1089 \(2016\)](#).
- [2] I. Pizorn, *Universality in entanglement of quasiparticle excitations*, [arXiv:1202.3336](#).
- [3] R. Berkovits, *Two-particle excited states entanglement entropy in a one-dimensional ring*, [Phys. Rev. B **87**, 075141 \(2013\)](#), [[arXiv:1302.4031](#)].
- [4] J. Mölter, T. Barthel, U. Schollwöck and V. Alba, *Bound states and entanglement in the excited states of quantum spin chains*, [J. Stat. Mech. \(2014\) 10029](#), [[arXiv:1407.0066](#)].
- [5] O. A. Castro-Alvaredo, C. De Fazio, B. Doyon and I. M. Szécsényi, *Entanglement Content of Quasiparticle Excitations*, [Phys. Rev. Lett. **121**, 170602 \(2018\)](#), [[arXiv:1805.04948](#)].
- [6] O. A. Castro-Alvaredo, C. De Fazio, B. Doyon and I. M. Szécsényi, *Entanglement content of quantum particle excitations. Part I. Free field theory*, [JHEP **10** \(2018\) 039](#), [[arXiv:1806.03247](#)].
- [7] O. A. Castro-Alvaredo, C. De Fazio, B. Doyon and I. M. Szécsényi, *Entanglement content of quantum particle excitations. Part II. Disconnected regions and logarithmic negativity*, [JHEP **11** \(2019\) 058](#), [[arXiv:1904.01035](#)].
- [8] O. A. Castro-Alvaredo, C. De Fazio, B. Doyon and I. M. Szécsényi, *Entanglement Content of Quantum Particle Excitations III. Graph Partition Functions*, [J. Math. Phys. **60**, 082301 \(2019\)](#), [[arXiv:1904.02615](#)].
- [9] J. Zhang and M. A. Rajabpour, *Excited state Rényi entropy and subsystem distance in two-dimensional non-compact bosonic theory. Part I. Single-particle states*, [JHEP **12** \(2020\) 160](#), [[arXiv:2009.00719](#)].
- [10] J. Zhang and M. A. Rajabpour, *Universal Rényi entanglement entropy of quasiparticle excitations*, [EPL **135**, 60001 \(2021\)](#), [[arXiv:2010.13973](#)].
- [11] J. Zhang and M. A. Rajabpour, *Corrections to universal Rényi entropy in quasiparticle excited states of quantum chains*, [J. Stat. Mech. \(2021\) 093101](#), [[arXiv:2010.16348](#)].
- [12] J. Zhang and M. A. Rajabpour, *Excited state Rényi entropy and subsystem distance in two-dimensional non-compact bosonic theory. Part II. Multi-particle states*, [JHEP **08** \(2021\) 106](#), [[arXiv:2011.11006](#)].
- [13] J. Zhang and M. A. Rajabpour, *Entanglement of magnon excitations in spin chains*, [JHEP **02** \(2022\) 072](#), [[arXiv:2109.12826](#)].

- [14] G. Mussardo and J. Viti, *The $\hbar \rightarrow 0$ limit of the entanglement entropy*, *Phys. Rev. A* **105**, 032404 (2022), [[arXiv:2112.06840](#)].
- [15] L. Capizzi, O. A. Castro-Alvaredo, C. De Fazio, M. Mazzoni and L. Santamaría-Sanz, *Symmetry resolved entanglement of excited states in quantum field theory. Part I. Free theories, twist fields and qubits*, *JHEP* **12** (2022) 127, [[arXiv:2203.12556](#)].
- [16] L. Capizzi, C. De Fazio, M. Mazzoni, L. Santamaría-Sanz and O. A. Castro-Alvaredo, *Symmetry resolved entanglement of excited states in quantum field theory. Part II. Numerics, interacting theories and higher dimensions*, *JHEP* **12** (2022) 128, [[arXiv:2206.12223](#)].
- [17] L. Capizzi, M. Mazzoni and O. A. Castro-Alvaredo, *Symmetry Resolved Entanglement of Excited States in Quantum Field Theory III: Bosonic and Fermionic Negativity*, [arXiv:2302.02666](#).
- [18] L. Amico, R. Fazio, A. Osterloh and V. Vedral, *Entanglement in many-body systems*, *Rev. Mod. Phys.* **80**, 517 (2008), [[arXiv:quant-ph/0703044](#)].
- [19] J. Eisert, M. Cramer and M. B. Plenio, *Area laws for the entanglement entropy - a review*, *Rev. Mod. Phys.* **82**, 277–306 (2010), [[arXiv:0808.3773](#)].
- [20] P. Calabrese, J. Cardy and B. Doyon, *Entanglement entropy in extended quantum systems*, *J. Phys. A: Math. Gen.* **42**, 500301 (2009).
- [21] N. Laflorencie, *Quantum entanglement in condensed matter systems*, *Phys. Rept.* **646**, 1 (2016), [[arXiv:1512.03388](#)].
- [22] E. Witten, *APS Medal for Exceptional Achievement in Research: Invited article on entanglement properties of quantum field theory*, *Rev. Mod. Phys.* **90**, 045003 (2018), [[arXiv:1803.04993](#)].
- [23] J. Zhang and M. A. Rajabpour, *Subsystem distances between quasiparticle excited states*, *JHEP* **07** (2022) 119, [[arXiv:2202.11448](#)].
- [24] M. A. Nielsen and I. L. Chuang, *Quantum Computation and Quantum Information*. Cambridge University Press, Cambridge, UK, 10th anniversary ed., 2010, [10.1017/CBO9780511976667](#).
- [25] J. Watrous, *The Theory of Quantum Information*. Cambridge University Press, Cambridge, UK, 2018, [10.1017/9781316848142](#).
- [26] M. M. Wolf, F. Verstraete, M. B. Hastings and J. I. Cirac, *Area Laws in Quantum Systems: Mutual Information and Correlations*, *Phys. Rev. Lett.* **100**, 070502 (2008), [[arXiv:0704.3906](#)].
- [27] J.-M. Stéphan, S. Furukawa, G. Misguich and V. Pasquier, *Shannon and entanglement entropies of one- and two-dimensional critical wave functions*, *Phys. Rev. B* **80**, 184421 (2009), [[arXiv:0906.1153](#)].
- [28] J. M. Stéphan, G. Misguich and V. Pasquier, *Rényi entropy of a line in two-dimensional Ising models*, *Phys. Rev. B* **82**, 125455 (2010), [[arXiv:1006.1605](#)].

- [29] D. J. Luitz, F. Alet and N. Laflorencie, *Universal Behavior beyond Multifractality in Quantum Many-Body Systems*, *Phys. Rev. Lett.* **112**, 057203 (2014), [[arXiv:1308.1916](#)].
- [30] D. J. Luitz, F. Alet and N. Laflorencie, *Shannon-Rényi entropies and participation spectra across three-dimensional $O(3)$ criticality*, *Phys. Rev. B* **89**, 165106 (2014), [[arXiv:1402.4813](#)].
- [31] D. J. Luitz, N. Laflorencie and F. Alet, *Participation spectroscopy and entanglement Hamiltonian of quantum spin models*, *J. Stat. Mech.* (2014) 08007, [[arXiv:1404.3717](#)].
- [32] Z.-Y. Dong and J.-X. Li, *Confinement and oscillating deconfinement crossover of two-magnon excitations in quantum spin chains quantified by spin entanglement entropy*, *Phys. Rev. B* **105**, L220402 (2022), [[arXiv:2206.08018](#)].
- [33] H. W. Lau and P. Grassberger, *Information theoretic aspects of the two-dimensional Ising model*, *Phys. Rev. E* **87**, 022128 (2013), [[arXiv:1210.5707](#)].
- [34] J.-M. Stéphan, *Emptiness formation probability, Toeplitz determinants, and conformal field theory*, *J. Stat. Mech.* (2014) 05010, [[arXiv:1303.5499](#)].
- [35] F. C. Alcaraz and M. A. Rajabpour, *Universal behavior of the Shannon mutual information of critical quantum chains*, *Phys. Rev. Lett.* **111**, 017201 (2013), [[arXiv:1305.1239](#)].
- [36] J.-M. Stéphan, *Shannon and Rényi mutual information in quantum critical spin chains*, *Phys. Rev. B* **90**, 045424 (2014), [[arXiv:1403.6157](#)].
- [37] F. C. Alcaraz and M. A. Rajabpour, *Universal behavior of the Shannon and Rényi mutual information of quantum critical chains*, *Phys. Rev. B* **90**, 075132 (2014), [[arXiv:1405.1074](#)].
- [38] F. C. Alcaraz and M. A. Rajabpour, *Generalized mutual information of quantum critical chains*, *Phys. Rev. B* **91**, 155122 (2015), [[arXiv:1501.02852](#)].
- [39] J. C. Getelina, F. C. Alcaraz and J. A. Hoyos, *Entanglement properties of correlated random spin chains and similarities with conformally invariant systems*, *Phys. Rev. B* **93**, 045136 (2016), [[arXiv:1511.00618](#)].
- [40] K. Najafi and M. A. Rajabpour, *Formation probabilities and Shannon information and their time evolution after quantum quench in the transverse-field XY chain*, *Phys. Rev. B* **93**, 125139 (2016), [[arXiv:1511.06401](#)].
- [41] F. C. Alcaraz, *Universal behavior of the Shannon mutual information in nonintegrable self-dual quantum chains*, *Phys. Rev. B* **94**, 115116 (2016), [[arXiv:1606.04994](#)].
- [42] B. Tarighi, R. Khasseh, M. N. Najafi and M. A. Rajabpour, *Universal logarithmic correction to Rényi (Shannon) entropy in generic systems of critical quadratic fermions*, *Phys. Rev. B* **105**, 245109 (2022), [[arXiv:2203.13124](#)].

- [43] V. E. Korepin, A. G. Izergin, F. H. L. Essler and D. B. Uglov, *Correlation function of the spin 1/2 XXX antiferromagnet*, *Phys. Lett. A* **190**, 182–184 (1994), [[arXiv:cond-mat/9403066](#)].
- [44] F. H. L. Essler, H. Frahm, A. G. Izergin and V. E. Korepin, *Determinant representation for correlation functions of spin 1/2 XXX and XXZ Heisenberg magnets*, *Commun. Math. Phys.* **174**, 191–214 (1995), [[arXiv:hep-th/9406133](#)].
- [45] F. H. L. Essler, H. Frahm, A. R. Its and V. E. Korepin, *Integrodifference equation for a correlation function of the spin 1/2 Heisenberg XXZ chain*, *Nucl. Phys. B* **446**, 448–460 (1995), [[arXiv:cond-mat/9503142](#)].
- [46] M. Shiroishi, M. Takahashi and Y. Nishiyama, *Emptiness formation probability for the one-dimensional isotropic XY model*, *J. Phys. Soc. Jpn.* **70**, 3535 (2001), [[arXiv:cond-mat/0106062](#)].
- [47] N. Kitanine, J. M. Maillet, N. A. Slavnov and V. Terras, *Emptiness formation probability of the XXZ spin- $\frac{1}{2}$ Heisenberg chain at $\Delta = \frac{1}{2}$* , *J. Phys. A: Math. Gen.* **35**, L385–L388 (2002), [[arXiv:hep-th/0201134](#)].
- [48] V. E. Korepin, S. Lukyanov, Y. Nishiyama and M. Shiroishi, *Asymptotic behavior of the emptiness formation probability in the critical phase of XXZ spin chain*, *Phys. Lett. A* **312**, 21–26 (2003), [[arXiv:cond-mat/0210140](#)].
- [49] F. Franchini and A. G. Abanov, *Asymptotics of Toeplitz determinants and the emptiness formation probability for the XY spin chain*, *J. Phys. A: Math. Gen.* **38**, 5069 (2005), [[arXiv:cond-mat/0502015](#)].
- [50] M. A. Rajabpour, *Formation probabilities in quantum critical chains and Casimir effect*, *EPL* **112**, 66001 (2015), [[arXiv:1512.01052](#)].
- [51] M. A. Rajabpour, *Finite size corrections to scaling of the formation probabilities and the Casimir effect in the conformal field theories*, *J. Stat. Mech.* (2016) 123101, [[arXiv:1607.07016](#)].
- [52] F. Ares and J. Viti, *Emptiness formation probability and Painlevé V equation in the XY spin chain*, *J. Stat. Mech.* (2020) 013105, [[arXiv:1909.01270](#)].
- [53] M. N. Najafi and M. A. Rajabpour, *Formation probabilities and statistics of observables as defect problems in free fermions and quantum spin chains*, *Phys. Rev. B* **101**, 165415 (2020), [[arXiv:1911.04595](#)].
- [54] F. Ares, M. A. Rajabpour and J. Viti, *Scaling of the Formation Probabilities and Universal Boundary Entropies in the Quantum XY Spin Chain*, *J. Stat. Mech.* (2020) 083111, [[arXiv:2004.10606](#)].
- [55] F. Ares, M. A. Rajabpour and J. Viti, *Exact full counting statistics for the staggered magnetization and the domain walls in the X Y spin chain*, *Phys. Rev. E* **103**, 042107 (2021), [[arXiv:2012.14012](#)].

- [56] D. F. V. James, P. G. Kwiat, W. J. Munro and A. G. White, *Measurement of qubits*, *Phys. Rev. A* **64**, 052312 (2001), [[arXiv:quant-ph/0103121](#)].
- [57] W. P. Su, J. R. Schrieffer and A. J. Heeger, *Solitons in polyacetylene*, *Phys. Rev. Lett.* **42**, 1698–1701 (1979).
- [58] W. P. Su, J. R. Schrieffer and A. J. Heeger, *Soliton excitations in polyacetylene*, *Phys. Rev. B* **22**, 2099–2111 (1980).
- [59] P. Jurcevic, B. P. Lanyon, P. Hauke, C. Hempel, P. Zoller, R. Blatt and C. F. Roos, *Quasiparticle engineering and entanglement propagation in a quantum many-body system*, *Nature* **511**, 202–205 (2014), [[arXiv:1401.5387](#)].
- [60] P. Jurcevic, P. Hauke, C. Maier, C. Hempel, B. P. Lanyon, R. Blatt and C. F. Roos, *Spectroscopy of Interacting Quasiparticles in Trapped Ions*, *Phys. Rev. Lett.* **115**, 100501 (2015), [[arXiv:1505.02066](#)].
- [61] J. Zhang, G. Pagano, P. W. Hess, A. Kyprianidis, P. Becker, H. Kaplan, A. V. Gorshkov, Z. X. Gong and C. Monroe, *Observation of a many-body dynamical phase transition with a 53-qubit quantum simulator*, *Nature* **551**, 601–604 (2017), [[arXiv:1708.01044](#)].
- [62] D. González-Cuadra, D. Bluvstein, M. Kalinowski, R. Kaubruegger, N. Maskara, P. Naldesi, T. V. Zache, A. M. Kaufman, M. D. Lukin, H. Pichler, B. Vermersch, J. Ye and P. Zoller, *Fermionic quantum processing with programmable neutral atom arrays*, *Proc. Nat. Acad. Sci.* **120**, e2304294120 (2023), [[arXiv:2303.06985](#)].
- [63] J.-S. Caux, *The Bethe Wavefunction*. Cambridge University Press, 2014, [10.1017/CBO9781107053885](#). [Translated from M. Gaudin, *La Fonction d'Onde de Bethe*. Masson, 1983.]
- [64] M. Karbach and G. Muller, *Introduction to the Bethe ansatz I*, *Comput. Phys.* **11**, 36 (1997), [[arXiv:cond-mat/9809162](#)].
- [65] M. Goldstein and E. Sela, *Symmetry-resolved entanglement in many-body systems*, *Phys. Rev. Lett.* **120**, 200602 (2018), [[arXiv:1711.09418](#)].
- [66] J. C. Xavier, F. C. Alcaraz and G. Sierra, *Equipartition of the entanglement entropy*, *Phys. Rev. B* **98**, 041106 (2018), [[arXiv:1804.06357](#)].